MIT Libraries | DSpace@MIT

MIT Open Access Articles

Jet physics from static charges in AdS space

Massachusetts Institute of Technology

Jet physics from static charges in AdS space

Yang-Ting Chien,[1] Matthew D. Schwartz,[1] David Simmons-Duffin,[1] and Iain W. Stewart[1,2]

[1]*Center for the Fundamental Laws of Nature, Harvard University, Cambridge, Massachusetts 02138, USA*
[2]*Center for Theoretical Physics, Massachusetts Institute of Technology, Cambridge, Massachusetts 02139, USA*

Soft interactions with high-energy jets are explored in radial coordinates which exploit the approximately conformal behavior of perturbative gauge theories. In these coordinates, the jets, approximated by Wilson lines, become static charges in Euclidean AdS. The anomalous dimension of the corresponding Wilson line operator is then determined by the potential energy of the charges. To study these Wilson lines we introduce a ''conformal gauge'' which does not have kinetic mixing between radial and angular directions, and show that a number of properties of Wilson lines are reproduced through relatively simple calculations. For example, certain nonplanar graphs involving multiple Wilson lines automatically vanish. We also discuss the linear growth of the charges' imaginary potential energy with separation, and a relationship between Wilson line diagrams and Witten diagrams.

I. INTRODUCTION

The richness of quantum chromodynamics is hidden in its deceptively simple Lagrangian $\mathcal{L} = -\frac{1}{4}F_{\mu\nu}^2 + \bar{q}i\slashed{D}q - m\bar{q}q$. At low energy, the theory has a mass gap $\sim \Lambda_{\mathrm{QCD}}$ and a discrete set of bound states. At high temperature it forms a quark-gluon plasma. At high energy, another phenomenon emerges: jets. The preference for producing collimated jets arises from logarithmic enhancement due to collinear and soft singularities. The cross section for production of quarks alone is not infrared-safe, but the cross section for production of jets, built from quarks accompanied by collinear and soft radiation, is a calculable and well-defined quantity.

Another way to think about jets is through Sudakov logs. For example, consider the mass of a jet m_J computed in perturbation theory, assuming massless quarks. At leading order, the distribution is singular, $d\sigma/dm_J^2 \propto \delta(m_J^2)$, since there is no radiation. At higher orders, the distribution contains terms like $\alpha_s \frac{1}{m_J^2} \ln \frac{m_J^2}{Q^2}$ where Q is a typical hard scale, like the jet energy. In terms of the integrated jet mass $R(m_J^2) = \int_0^{m_J^2} dm'^2 (d\sigma/dm'^2)$, the series has the structure

$$R(m_J^2) = 1 + \alpha_s \ln^2 \frac{m_J^2}{Q^2} + \alpha_s^2 \ln^4 \frac{m_J^2}{Q^2} + \cdots \quad (1)$$

The coefficients of these terms and the precise definition of Q depend on the particular process, and for simplicity, we have only shown the leading large logarithms. These logs are Sudakov double logs, of the form $\alpha_s^n \ln^{2n} x$. They come from the region of overlapping soft and collinear divergences and are present in any gauge theory with massless charged particles. Sudakov logs invalidate the perturbation expansion. However when one resums the series, the final nonperturbative expression, schematically $R(m_J^2) = \exp(-\alpha_s \ln^2 \frac{m_J^2}{Q^2})$ vanishes at $m_J^2 = 0$ implying that the cross

section for producing massless quarks is zero. The objects that are produced are jets, of finite mass. The coefficient of the Sudakov log in this exponential is a function of the coupling constant $\Gamma_{\mathrm{cusp}}(\alpha_s)$ called the cusp-anomalous dimension.

Sudakov logs and the cusp-anomalous dimension are simplest to study in the soft limit of QCD, where one treats a massless parton (quark or gluon) as a hard charged object plowing through a background of soft radiation. The soft radiation cannot change the direction or energy of the hard parton, and so the parton factorizes out as a Wilson line source for soft gluons. This treatment of soft radiation becomes manifest when using QCD factorization theorems to describe hard collisions, see the reviews [1,2], or when using soft-collinear effective theory (SCET) [3–7] to describe the interaction of soft and collinear partons in hard collisions. Thus using Wilson line operators the soft interaction properties of jets can be investigated. Wilson lines also appear in the study of scattering in planar $\mathcal{N} = 4$ SYM, via a surprising duality relating null polygonal loops to scattering amplitudes [8–15].

A Wilson line is defined as

$$\mathcal{W}(C) = \mathcal{P} \exp\left(ig \int_C A_\mu dx^\mu\right), \quad (2)$$

where C is a contour describing the path of the partons and $\mathcal{P}$ denotes path-ordering along the contour. Typically, one takes C to be a simple closed contour, and makes $\mathcal{W}$ gauge-invariant by taking a trace. We will be creating gauge invariants using $\mathcal{W}$ in more complicated ways. For example, a process like $e^+e^- \to$ hadrons is, to leading order in α_s, described by $e^+e^- \to \bar{q}q$ with the quarks traveling off in the $n_1^\mu = (1, \vec{v})$ and $n_2^\mu = (1, -\vec{v})$ directions. In this case, we can write $\mathcal{W}(C)$ as the product of two Wilson lines from 0 to ∞ along n_1 and n_2, with one in the fundamental and one in the antifundamental representation.

More generally, for N-jet production in e^+e^- collisions or $(N-2)$-jet production in pp or $p\bar{p}$ collisions, we are interested in a product of N Wilson lines along directions n_i^μ,

$$\mathcal{W}_{d_1,\ldots,d_N}(n_1,\ldots,n_N)$$
$$= t_{c_1,\ldots,c_N}\prod_{i=1}^{N}\left(\mathcal{P}\exp ig\int_0^\infty dsn_i\cdot A^a(sn_i)\boldsymbol{T}_i^a\right)_{d_i}^{c_i}. \quad (3)$$

The lines here are all outgoing. For an incoming Wilson line we simply replace the path-ordering, $\mathcal{P}$, by anti-path-ordering, $\bar{\mathcal{P}}$, and replace the ig with $-ig$. Let us take a moment to explain the remaining notation. The $\boldsymbol{T}_i$ are gauge generators in the color representation R_i associated with parton i. They satisfy $[\boldsymbol{T}_i,\boldsymbol{T}_j]=0$ for $i\neq j$, along with the color conservation relation $\sum_i\boldsymbol{T}_i=0$. For light quarks and gluons the directions n_i^μ are lightlike, $n_i^2=0$, while for heavy quarks like the top where mass effects are important, we have $n_i^2\neq 0$. To keep our discussion general we will mostly work with $n_i^2\neq 0$. Often in the literature the timelike component of n_i^μ is taken to be positive, and the integration along the path extends from $s=0$ to ∞ for outgoing partons and from $s=-\infty$ to 0 for incoming partons. For simplicity we will always take $s=0$ to ∞ and let n_i^μ have a negative timelike component for incoming particles.[1]

$\mathcal{W}$ depends on a tensor $t_{c_1,\ldots,c_N}$, where the c_i denote the color indices at $s=0$. These tensors live in the color-invariant subspace $\mathcal{I}$ of the tensor product of representations associated with each jet

$$\mathcal{I}=(R_1\otimes R_2\otimes\ldots\otimes R_N)_{\text{color singlet subspace}}. \quad (4)$$

In a scattering process, the short-distance physics at the origin specifies the relevant channels and determines the $t_{c_1,\ldots,c_N}$, which are Clebsch-Gordan coefficients.

The d_i indices on Eq. (3) denote the color indices at $s=\infty$. Matrix elements of $\mathcal{W}(n_i)$ will be infrared-divergent unless the d_i are contracted, as in various physical calculations. For example, Wilson line matrix elements contribute to matching calculations in SCET, see e.g. [4,16–20]. Operators describing the hard interaction for N-jet production appear in the SCET Lagrangian as

$$\mathcal{L}=C_{c_1,\ldots,c_N}(s_{ij})\mathcal{O}^{c_1,\ldots,c_N}(n_i)$$
$$=C(s_{ij})[\chi_{n_j}^{d_j}\cdots\bar{\chi}_{n_k}^{d_k}\cdots\mathcal{B}_{n_\ell}^{\perp d_\ell}\ldots]\mathcal{W}_{d_j,\cdots,d_k,\cdots,d_\ell,\cdots}(n_i), \quad (5)$$

where $C_{c_1,\ldots,c_N}(s_{ij})=t_{c_1,\ldots,c_N}C(s_{ij})$ is a Wilson coefficient depending on hard scales $s_{ij}=p_i\cdot p_j$, where $p_i=n_iQ_i$ are the jet four-momenta at leading power (and in general

we have a sum over terms of this sort for the possible color structures $t_{c_1,\ldots,c_N}$). In square brackets are collinear quark (χ_{n_j}) and gluon ($\mathcal{B}_{n_\ell}^\perp$) fields that are each contracted in color with the d_j or d_ℓ indices from the Wilson line. In a matching computation the infrared divergences from matrix elements of collinear fields and from the soft Wilson lines combine to yield the same infrared divergences as for the corresponding matrix element in QCD, ensuring that the Wilson coefficients $C(s_{ij})$ are finite. In this computation there is a cancellation of overlapping infrared and ultraviolet divergences between the collinear matrix elements and matrix elements involving the soft Wilson lines.

Alternatively, the Wilson line can be used to calculate a soft function (for examples see [19,21–28]), which appear in physical cross sections for hard processes with jet production

$$S(k)=\langle 0|\mathcal{W}_{d_1,\cdots,d_N}(n_i)\hat{M}(k)\mathcal{W}_{d_1,\cdots,d_N}^\dagger(n_i)|0\rangle. \quad (6)$$

In this case, the d_i indices of the Wilson line are contracted with those of its adjoint and the product includes a measurement function $M(k)$ which acts on final-state soft partons, measuring momentum components k. These soft functions are cross sections for soft radiation and are infrared-finite by themselves.

An important property of Wilson lines is that, even though they are nonlocal objects, they are multiplicatively renormalizable. A number of *features* are known (or conjectured) about the renormalization of $\mathcal{W}(C)$.

(1) If the contour C is smooth and not self-intersecting, any ultraviolet divergences in correlators of $\mathcal{W}(C)$ are exactly canceled by field strength and coupling constant counterterms.[2] For the $\mathcal{W}(n_i)$ relevant for jet physics, the Wilson line has kinks and self-intersections in its path at the origin, and C is not smooth. In this case additional divergences are present and the Wilson line picks up an anomalous dimension Γ. This anomalous dimension can only depend on the angles β_{ij} where the contour abruptly changes direction or on crossing angles at self-intersections [29]. When the direction of the contour changes from n_i^μ to n_j^μ, the *cusp angle* is

$$\cosh\beta_{ij}=\frac{n_i.n_j}{|n_i||n_j|}, \quad (7)$$

where here we consider paths where $|n_i|^2=n_i^2\neq 0$. For two jets from $e^+e^-\to q\bar{q}$ (with massive quarks), β_{12} is real. More generally, for $e^+e^-\to N$ jets, all the n_i^μ correspond to final-state jets and each β_{ij} is real.

---

[1]Another common convention in the literature is to use tangent vectors to the contour v_i^μ, in place of our n_i^μ. For a 2-jet Wilson line for $e^+e^-\to q\bar{q}$, the relation to our conventions is $v_1=-n_1$ to $v_2=n_2$, where n_1 and n_2 have positive time-components.

[2]At least this is the case in dimensional regularization. More generally, there can be an overall linear divergence proportional to the length of the Wilson line, which can also be subtracted off with an appropriate counterterm.

(2) At order α_s, the anomalous dimension is

$$\Gamma = -\frac{\alpha_s}{\pi}\sum_{i<j}\boldsymbol{T}_i\cdot\boldsymbol{T}_j((\beta_{ij} - i\pi)\coth\beta_{ij} - 1), \quad (8)$$

where the sum is over pairs of jet directions n_i, n_j. The color structure $\boldsymbol{T}_i\cdot\boldsymbol{T}_j\equiv T_i^a T_j^a$ involves the generators from Eq. (3). These generators allow the anomalous dimension Γ to mix the different invariant tensors t_{c_i} in Eq. (3) during renormalization group flow. Γ is an operator on the space I, which we can write as a general expression with generators $\boldsymbol{T}_i$ acting on the ith tensor factor.

(3) In situations like jet production in hadron collisions or deep inelastic scattering (DIS), there are both initial-state and final-state Wilson lines. Initial-state Wilson lines follow paths that extend backward in time from the origin, $n^\mu = (-1, \vec{v})$. For cusps between initial- and final-state partons β_{ij} is complex, but we can define a real cusp angle $\gamma_{ij} = \beta_{ij} - i\pi$. This alternative definition of the cusp angle is related to the previous one by a sign

$$\cosh\gamma_{ij} = -\frac{n_i\cdot n_j}{|n_i||n_j|} = -\cosh\beta_{ij}, \quad (9)$$

The angles β_{ij} and γ_{ij} are illustrated in Fig. 1. Whether γ_{ij} or β_{ij} are complex affects the complexity of the anomalous dimension, which has physical consequences. For example, these factors of $i\pi$ can partly explain the large K-factor in the Higgs production cross section [30].

(4) *Abelian exponentiation*: The anomalous dimension in QED without propagating quarks is one-loop exact.

(5) In the limit that the tangent vectors become light-like, $n_i^2 \to 0$ and $\beta_{ij} \to \infty$, the anomalous dimension becomes *linear* in the cusp angles β_{ij} to all orders in perturbation theory [29,31,32],
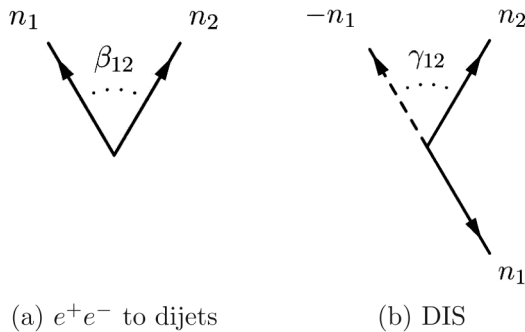

(a) e^+e^- to dijets   (b) DIS

FIG. 1.   Our definitions for the cusp angles β_{12} and γ_{12}. β_{12} is real when both Wilson lines represent final-state partons, while γ_{12} is real when one Wilson line represents a final-state parton, and one represents an initial-state parton.

$$\Gamma = -\sum_{i<j}\Gamma^{ij}(\alpha_s)\beta_{ij} + \dots \quad (10)$$

where "…" are terms that are constant or go to zero as $\beta_{ij} \to \infty$. The possibility that $\Gamma^{ij}(\alpha_s) = \boldsymbol{T}_i\cdot\boldsymbol{T}_j\Gamma_{\text{cusp}}(\alpha_s)$, where $\Gamma_{\text{cusp}}(\alpha_s)$ is independent of i and j, is known as *Casimir scaling*. This has been shown by explicit calculations for two lines at three loops [33], and by other arguments for multiple lines up to four loops [24].

Exactly at $n_i^2 = 0$, $\beta_{ij} = \infty$ and the anomalous dimension is singular. This singularity is due to additional overlapping soft and collinear divergences, and induces dependence of the anomalous dimension on the renormalization group scale μ. For example, at one loop,

$$\Gamma = \frac{\alpha_s}{\pi}\sum_{i<j}\boldsymbol{T}_i\cdot\boldsymbol{T}_j\ln\frac{\mu^2}{n_i\cdot n_j\Lambda^2} + \dots. \quad (11)$$

Here Λ is another scale with dimension of mass. In matrix elements of Wilson lines, which are infrared-divergent, Λ is related to the infrared regulator. When collinear graphs are included in the calculation of Wilson coefficients for a hard scattering process, as in Eq. (5), the infrared regulator will cancel and Λ will be replaced by a hard scale $\Lambda^2 \to \pm Q_i Q_j$. In calculating soft functions, as in Eq. (6), the infrared divergences will cancel between real and virtual contributions, and the scale will be replaced by a physical one, relevant to the soft function $\Lambda^2 \to k_i k_j$. At all orders, the anomalous dimension is linear in $\ln\mu^2$, for the same reason that Γ is linear in β_{ij} at large cusp angles. Proofs of Eq. (10) for two Wilson lines have been given in Refs. [16,31,34], and for multiple lines in Refs. [24,35,36].

(6) At one loop the anomalous dimension must be a sum over pairs of Wilson lines. Surprisingly some pairwise structure seems to persist to higher orders in perturbation theory. For example, in the massless case, the anomalous dimension of a 4-jet Wilson line at two loops, as a matrix in color space, was found to be exactly proportional to the one-loop anomalous dimension, an unexpected result [37].

It has been conjectured that for massless jets the anomalous dimension of the N-jet Wilson line has a pairwise structure to all orders in perturbation theory for the $\ln\mu$ term [24,36,38–40]

$$\Gamma \stackrel{?}{=} \sum_{i\neq j}\Gamma_{\text{cusp}}^{ij}(\alpha_s)\boldsymbol{T}_i\cdot\boldsymbol{T}_j\ln\frac{\mu^2}{n_i\cdot n_j\Lambda^2}$$
$$+ \gamma(\alpha_s, \{n_k\cdot n_\ell\}). \quad (12)$$

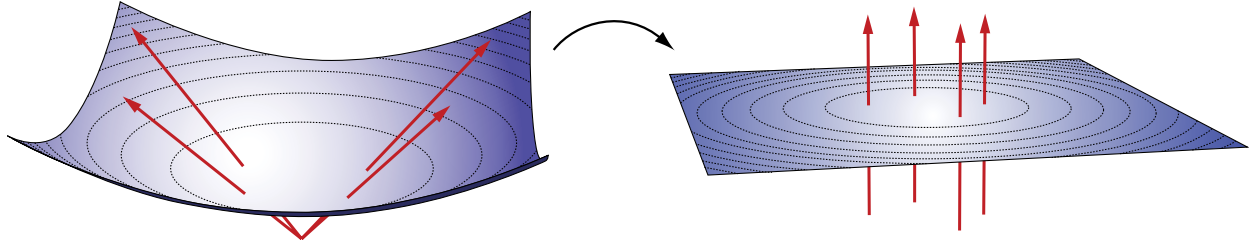Given Eq. (10) and (12) becomes nontrivial for four or more Wilson lines where matrices appear for the

FIG. 2 (color online).   A coordinate change maps Minkowski space to $\mathbb{R} \times$ AdS. In this figure the outgoing Wilson lines become static charges in AdS, and their tree level energy in AdS is equal to the original one-loop anomalous dimension for the lines.

color structures. If there were a general proof of Casimir scaling it would imply that $\Gamma_{\text{cusp}}^{ij}(\alpha_s)$ cannot depend on the representations i and j, making the coefficient a universal function $\Gamma_{\text{cusp}}^{ij}(\alpha_s) = \Gamma_{\text{cusp}}(\alpha_s)$. This was conjectured in [24,38].

It has been furthermore conjectured that the regular anomalous dimension γ is independent of conformal cross ratios (combinations of cusp angles $\beta_{ij} + \beta_{k\ell} - \beta_{ik} - \beta_{j\ell}$ that approach nontrivial constants as the $\beta_{ij} \to \infty$), so that [24]

$$\gamma(\alpha_s, \{n_i \cdot n_j\}) \overset{?}{=} \sum_i \gamma^i(\alpha_s). \qquad (13)$$

This is known to be true to $\mathcal{O}(\alpha_s^2)$. At $\mathcal{O}(\alpha_s^3)$ and beyond general constraints on the form of $\gamma(\alpha_s, \{n_i \cdot n_j\})$ were reviewed in Ref. [24,41]. Dependence on conformal cross ratios appears not to be forbidden by symmetry arguments, but whether this dependence exists is an open question. Possible terms at $\mathcal{O}(\alpha_s^3)$ which were not obviously forbidden were suggested in Ref. [41]. Very recently it was argued that these terms are forbidden by considerations from the Regge limit in Refs. [42,43].

Most of these results have been shown only through direct, and sometimes laborious calculations. Even a simple result, such as Abelian exponentiation, requires the use of eikonal identities and monitoring of combinatoric factors. In this paper, we will show how some of these results can be understood in a simple way using a mapping inspired by the approximate conformal invariance of QCD.

At the classical level, QCD is conformally invariant. This symmetry is broken by quantum effects, but for high-energy scattering it continues to have implications for the structure of perturbative results. Examples of the implications of conformal symmetry for QCD can be found in Refs. [32,44–48]. Our main focus here will be on exploiting conformal invariance to understand properties of the anomalous dimensions of Wilson lines relevant for jet physics.

A Wilson line emanating from the origin in the direction n^μ comprises the points $x^\mu = sn^\mu$, for $s > 0$. A scale

transformation is simply a change in s. Scale invariance is made more manifest by defining a new time coordinate $\tau \equiv \ln|x|$ where $|x|$ is the (Lorentzian) distance from the origin. This makes the Wilson lines parallel, as shown in Fig. 2. In terms of τ, rescaling becomes simply time translation, and conformal symmetry becomes the statement that the physics is time-translation-invariant in τ. The Wilson lines become static charges whose energy is the anomalous dimension. Spatial slices in these coordinates are copies of Euclidean anti-de Sitter space (AdS). In this paper, we describe how many of the features of Wilson lines enumerated above can be understood in AdS coordinates. For example, that the Coulomb potential is one-loop exact in QED automatically implies that the anomalous dimension of multiple Wilson line operators are one-loop exact in QED.

In addition to providing a pleasing physical picture, radial coordinates make a number of calculations much easier. One of the reasons that the classical conformal invariance of QCD rarely simplifies diagrammatic computations is that it is broken by standard gauge choices, such as Feynman gauge. Feynman gauge in flat space leads to kinetic mixing between the timelike components A_τ and spacelike components A_i of the gauge field in $\mathbb{R} \times$ AdS. Here we introduce a new gauge, which we call *conformal gauge*, in which there is no such mixing. One consequence is that in this gauge, since only A_τ is sourced by the Wilson lines, and there is no A_τ^3 or A_τ^4 vertex in Yang-Mills theory, many of the nonplanar graphs at two and three loops automatically vanish. This automatically implies that the only graphs at two loops contributing to the anomalous dimension have gluons going between pairs of Wilson lines, which strongly suggests a pairwise structure. This reasoning alone does not imply that Γ must be pairwise at three loops or higher.

The organization of this paper is as follows. In Sec. II we discuss the appropriate mapping of Minkowski to AdS coordinates and simple implications for multi-Wilson line configurations. In Sec. III we compute the one-loop anomalous dimension of $\mathcal{W}$ by carrying out a classical energy computation in AdS, paying special attention to boundary conditions and differences for incoming and outgoing lines. We repeat this computation using the

standard one-loop diagrams in Sec. IV, but utilizing the AdS coordinates. A discussion of the lightlike limit and a way to think about the imaginary energy in AdS is given in Sec. V. In Sec. VI, we introduce conformal gauges which do not mix the time and spatial components of the gauge boson propagator in $\mathbb{R} \times$ AdS, and in Sec. VII we demonstrate the utility of such gauges by computing a two-loop contribution to the anomalous dimension of $\mathcal{W}$ in a simple way. In Sec. VIII, we mention an interesting formal relation between anomalous dimension calculations for $\mathcal{W}$ and Witten diagrams. We conclude in Sec. IX. Several technical discussions are relegated to appendices. In App. A we construct the most general class of conformal gauges without auxiliary parameters, and in App. B we give the corresponding Feynman rules for ghosts.

II. CONFORMAL COORDINATES

Having replaced hard partons by Wilson lines, the soft physics is described simply by Yang-Mills theory, which enjoys classical conformal invariance in four dimensions. Equivalently, the soft action coupled to a background metric $g_{\mu\nu}$ is Weyl-invariant: it is unchanged under a local rescaling of the metric, $S_{\mathrm{YM}}[g] = S_{\mathrm{YM}}[e^{2\omega(x)}g]$. Although this symmetry is broken by fermion masses and the QCD scale anomaly that generates Λ_{QCD}, it continues to have important implications for scattering amplitudes at high energies.

One reason conformal invariance can be useful for QCD is that some quantities are completely insensitive to the breaking of conformal invariance. For example, the one-loop cusp-anomalous dimension Eq. (8) is independent of the matter content of the theory, since Feynman diagrams contributing to it only involve a single gluon exchanged between Wilson lines. Consequently, it has a universal form, and we can compute it assuming exact conformal invariance. In other words, we can compute it in our favorite conformal theory, for instance $\mathcal{N} = 4$ SYM, and the result will hold in any gauge theory. In the next two sections, we will use this fact to give a simple and intuitive derivation of Eq. (8).

To the extent that conformal symmetry is a good approximation, it is natural to apply techniques which have proved useful for studying conformal field theories in other contexts. In particular, we consider *radial quantization* around the origin. In Ref. [8] this was used to study the anomalous dimensions of high spin operators, and has also been used in Ref. [44]. In this section, we review the relevant ideas in the context of N-jet Wilson lines.

Consider a Wilson line in the direction n^μ. We can write $n^\mu = (\cosh\beta, \sinh\beta\hat{\mathbf{n}})$, with $\hat{\mathbf{n}}$ a unit vector in $\mathbb{R}^3$, and $x^\mu = e^\tau n^\mu$. The path of the Wilson line is then described by

$$t = e^\tau \cosh\beta, \qquad r = e^\tau \sinh\beta, \qquad \beta, \theta, \phi \text{ fixed,} \tag{14}$$

with τ running from $-\infty$ to ∞. Wilson lines in different directions will correspond to different values of β, θ and ϕ. In these coordinates, the Minkowski metric becomes

$$ds^2_{\mathbb{R}^{1,3}} = dt^2 - dr^2 - r^2 d\Omega_2^2$$
$$= e^{2\tau}[d\tau^2 - (d\beta^2 + \sinh^2\beta d\Omega_2^2)]. \tag{15}$$

Strictly speaking, this metric describes only a patch of $\mathbb{R}^{1,3}$—namely the interior of the future light cone. We will return to this point shortly.

The idea of radial quantization is to interpret τ as a new time coordinate. A naïve complication in this picture is that the metric Eq. (15) is now time-dependent. However, in a conformal theory, the dynamics is independent of the local scale, and we can equivalently consider our theory with any metric related via $ds^2 \to e^{2\omega(x)}ds^2$. Thus, let us drop the overall $e^{2\tau}$ to obtain a simple time-translation-invariant product space,

$$ds^2_{\mathbb{R}\times\mathrm{AdS}} = d\tau^2 - (d\beta^2 + \sinh^2\beta d\Omega_2^2). \tag{16}$$

The spatial part of this metric is the 3D hyperboloid, or Euclidean anti-de Sitter space. With a slight abuse of nomenclature, we call it simply AdS.

In radial coordinates, the origin maps to $\tau = -\infty$ and motion along a Wilson line corresponds to shifts in τ. So to the extent that our theory was scale-invariant in Minkowski space, it is now time-translation-invariant in $\mathbb{R} \times$ AdS. Each Wilson line sits at fixed (β, θ, ϕ) and extends from $-\infty$ to ∞ in the time coordinate τ. That is, each Wilson line becomes a static charge in AdS. For perturbative computations in QCD (where conformal invariance is broken by the scale anomaly) we may simply adopt the change of coordinates in Eq. (14) as a method to carry out computations. If the computation involves ingredients satisfying the conformal invariance then the factors of e^τ will cancel out, and the result will be constrained by properties of the AdS space.

For the sake of doing calculations, a key point is that the dilatation operator in Minkowski space maps to the Hamiltonian in AdS in radial quantization

$$\mathcal{D}^{\mathbb{R}^{1,3}} = x^\mu \partial_\mu = \partial_\tau = i\mathcal{H}^{\mathbb{R}\times\mathrm{AdS}}. \tag{17}$$

Consequently, the eigenvalue of dilatation—the dimension (or when acting on classically scale-invariant Wilson lines, the anomalous dimension)—is just i times the energy in AdS. So we can calculate anomalous dimensions by calculating energies and apply our intuition from electrodynamics to understand anomalous dimensions of Wilson lines.

What can the energy of two static charges in AdS depend on? Since the space is homogeneous, it can depend only on the geodesic distance between the charges. For example, suppose we have two timelike Wilson lines, pointing in the directions n_1^μ and n_2^μ, normalized so that $n_1^2 = n_2^2 = 1$. We may first go to the rest frame of one, $n_1^\mu = (1, 0, 0, 0)$, and

then rotate so the other is at $n_2^\mu = (\cosh\beta_{12}, \sinh\beta_{12}, 0, 0)$. Then the geodesic distance between them, using the spatial part of the metric Eq. (16), is just

$$\Delta s = \beta_{12}. \qquad (18)$$

Considering also that $\frac{n_1 \cdot n_2}{|n_1||n_2|} = \cosh\beta_{12}$, we see that the geodesic distance in AdS is the cusp angle. Thus, the energy of the two charges, and hence the anomalous dimension in Minkowski space, can depend only on the cusp angle. This was *feature 1* from the introduction. More succinctly, the original Lorentz symmetry of Minkowski space becomes the isometry group of AdS in radial coordinates. Just as Lorentz invariance dictates that the anomalous dimension can depend only on the cusp angle, the isometries of AdS dictate that the energy can depend only on the geodesic distance.

We can also consider initial-state Wilson lines. For example, in deep inelastic scattering as Bjorken $x \to 1$, the initial state contains an energetic proton in the Breit frame, the final state contains a jet, and the Wilson line description applies. In our convention, the spatial vectors for these lines still point out from the origin, and the lines extend to negative Minkowski times. Instead of Eq. (14), the path of an initial-state line is then described by

$$t = -e^\tau \cosh\gamma, \qquad r = e^\tau \sinh\gamma, \qquad (19)$$

for fixed real γ. When comparing the coordinates for parallel initial- and final-state lines we have $\hat{n} \to -\hat{n}$ so $\theta \to \theta + \pi$ and $\phi \to \phi + \pi$. In radial quantization, initial-state lines map to static charges in a different copy of $\mathbb{R} \times \text{AdS}$ comprising points in the interior of the past light cone (Fig. 3). It is useful to think of this second copy of AdS as being related by analytic continuation to the first. Since from Eq. (9) we have $\cosh\gamma = -\cosh\beta$, we can write $\beta = \gamma + i\pi$. Both copies of AdS (along with a copy of de Sitter space describing points at spacelike separation from the origin) are related by analytic continuation to the three-sphere S^3 that one would obtain by repeating the exercise of radial quantization starting from Euclidean space, $\mathbb{R}^4$. This will be a useful tool in the following section.

For most of the remainder of the paper, we will focus on timelike Wilson lines whose directions are normalized to $n^2 = 1$. Since all the energies and dimensions are independent of rescaling of the n's, the dependence on $|n|$ can be put back by dimensional analysis: $n_i^\mu \to \frac{n_i^\mu}{|n_i|}$. We will also have occasion to consider the lightlike limit $n^2 \to 0$, which is phenomenologically relevant for the majority of processes at colliders. Many of the properties of the lightlike case can be derived as a limiting case of the general timelike results. In the lightlike limit $n_i^2 \to 0$, and the charges move towards the boundary of AdS with $\beta \to \infty$. Some results simplify for $n^2 = 0$, and when appropriate we will consider this case separately.
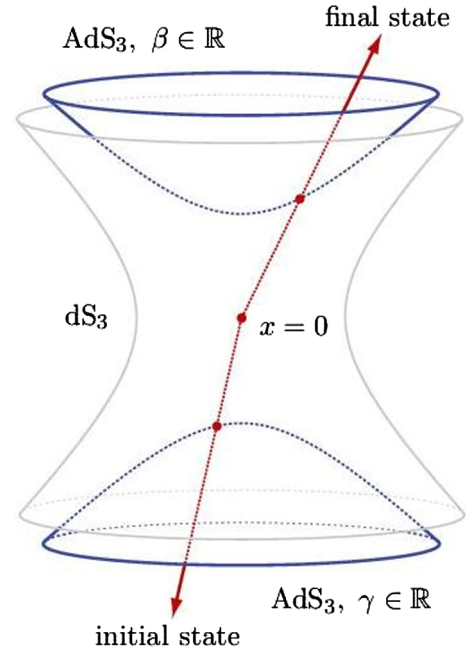

FIG. 3 (color online).   In radial quantization, final-state lines map to a copy of AdS_3 at positive Minkowski times, while initial-state lines map to a second copy of AdS_3 at negative Minkowski times. Points that are spacelike separated from the origin map to dS_3.

III. CLASSICAL ADS ENERGIES

In radial coordinates, we have seen that the anomalous dimension of a collection of Wilson lines intersecting at a point is proportional to the energy of a collection of static charges in AdS. This energy can only depend on the geodesic distance between the charges, which is the same as the cusp angle $\beta_{ij} = \cosh^{-1} n_i \cdot n_j$. Now let us calculate that energy.

The energy of two charges in QCD at leading order is given, as in QED, by solving Laplace's equation for the scalar potential A_τ in the presence of point sources J_μ given by $J_\tau = \delta^3(x)$ and $\vec{J} = 0$. The homogeneous solutions are

$$\frac{1}{\sinh^2\beta} \partial_\beta(\sinh^2\beta(\partial_\beta A_\tau)) = 0 \Rightarrow A_\tau(\beta)$$

$$= C_1 + C_2 \coth\beta. \qquad (20)$$

Unfortunately, neither of these is the physically correct answer. This can be seen most easily by looking at the large β limit, where we expect $A_\tau(\beta)$ to be linear in β. In this limit Eq. (20) behaves as a constant.

The problem with this potential is that it has the wrong boundary conditions. This is easiest to understand by analytically continuing to Euclidean space. Defining $\beta = i\alpha$, the metric becomes

$$ds^2 = d\tau^2 + d\alpha^2 + \sin^2(\alpha)d\Omega_2^2 = d\tau^2 + d\Omega_3^2, \qquad (21)$$

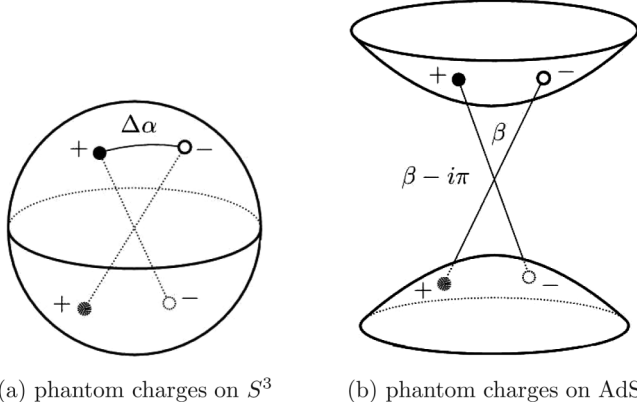(a) phantom charges on S^3 (b) phantom charges on AdS

FIG. 4. The naive solution to Laplace's equation on the Euclidean cylinder, Eq. (22), represents the potential in the presence of additional phantom charges at diametrically opposite points on the sphere, Fig. 4(a). After analytic continuation back to Minkowski signature, the phantom charges map to another copy of AdS, Fig. 4(b), corresponding to phantom initial-state particles.

which describes a Euclidean cylinder $\mathbb{R} \times S^3$. The Wilson lines are now static charges at points on a three-sphere. The general homogeneous solution to Laplace's equation on $\mathbb{R} \times S_3$ is the analytic continuation of Eq. (20)

$$A_\tau(\alpha) = C_1 + C_2 \cot\alpha. \qquad (22)$$

Since $\cot\alpha$ has a pole at both $\alpha = 0$ and $\alpha = \pi$, Eq. (22) actually describes a configuration with two charges: a $(+)$ charge at the north pole and a phantom $(-)$ charge at the south pole. If we now consider two physical charges separated by an angle $\Delta\alpha$ on the sphere, we obtain a potential for not just these two charges, but also for two additional phantom charges, which is incorrect. This is shown graphically in Fig. 4(a). The AdS version is shown in Fig. 4(b) and discussed more below.

A nice way to get the correct solution to Laplace's equation on the Euclidean cylinder is to add and subtract a constant charge density. On the Euclidean cylinder, a point charge should correspond to the source current $J_\tau = \delta^3(x)$. Instead, we take $J_\tau(x) = \delta^3(x) - \frac{1}{2\pi^2}$ which has a point charge at $x = 0$ but is neutral overall. If we linearly combine such charge densities to construct an overall neutral collection of point charges, the constant parts of the charge density will exactly cancel, but the phantom charges will be absent. The solution to Laplace's equation on the Euclidean cylinder with this current is

$$A_\tau^{\text{Eucl.}}(\alpha) = \frac{1}{4\pi^2}(\pi - \alpha)\cot\alpha + \text{constant}, \qquad (23)$$

where the constant is an overall energy which is not yet fixed. This same result was computed earlier in Ref. [44] by computing the transition amplitude by summing over classical paths, and performing an infinite sum of SU(2) characters.

The quantity $A_\tau(\alpha)$ in Eq. (23) is the scalar potential on the sphere due to one charge, assuming an overall neutral distribution. To calculate the total energy for two charges $q_1 = -q_2$ separated by a distance α_{12}, we can compute

$$E_{\text{pair}}^{\text{Eucl.}}(\alpha_{12}) = \frac{1}{2}\int_{\Omega_3}(\vec{E}_1 + \vec{E}_2)^2, \qquad (24)$$

where $\vec{E}_{1,2} = \vec{\nabla}(qA_\tau)_{1,2}$ is the electric field due to each charge. Integrating by parts, using the equations of motion, and throwing away the infinite self-energy of each charge, this is just

$$E_{\text{pair}}^{\text{Eucl.}}(\alpha_{12}) = q_1 q_2 A_\tau(\alpha_{12}) + \text{constant}. \qquad (25)$$

Already, the reader may recognize $E_{\text{pair}}^{\text{Eucl.}}(\alpha)$ as the α-dependent part of the cusp-anomalous dimension in Euclidean space.

The equivalent of this calculation in AdS gives

$$E_{\text{pair}}(\beta_{12}) = \frac{q_1 q_2}{4\pi^2}[(\pi + i\beta_{12})\coth\beta_{12} + C]. \qquad (26)$$

Here C is an undetermined constant setting the zero of energy, which must be fixed by other considerations. When both Wilson lines are outgoing, as in the process $e^+ e^- \to q\bar{q}$, β_{12} is real and positive. At small β, the charges become closer than the curvature scale, and the energy reduces to

$$E_{\text{pair}}(\beta_{12}) \to \frac{q_1 q_2}{4\pi}\frac{1}{\beta_{12}}. \qquad (27)$$

This is the correct behavior of the energy of two charges as a function of geodesic separation. Unfortunately, setting $\beta = 0$ is singular, so this limit cannot be used to determine the constant C.

When one Wilson line is outgoing and one is incoming, as in DIS, there is a smooth limit to zero separation which can be used to fix C. In this configuration, the quantity $\gamma = \beta - i\pi$ is real. Expressing the energy in terms of γ_{12}, we obtain

$$E_{\text{pair}}(\gamma_{12}) = i\frac{q_1 q_2}{4\pi^2}(\gamma_{12}\coth\gamma_{12} - iC). \qquad (28)$$

In this case, the limit $\gamma_{12} = 0$ is physical: it corresponds to our two Wilson lines reducing to a single straight line going from $t = -\infty$ to $t = +\infty$ through the origin. This contour has no cusp and is in fact a conserved current (occurring in the Isgur-Wise function [49]), so its anomalous dimension must vanish. This determines the boundary condition $E_{\text{pair}}(\gamma_{12} = 0) = 0$, which sets $C = -i$.

In summary, restoring the color factors, charges, and coupling constant for QCD, and summing over pairs of charges to compute the total energy, we have found

$$E_{\text{tot}} = \frac{i\alpha_s}{\pi}\sum_{i<j}\boldsymbol{T}_i \cdot \boldsymbol{T}_j[(\beta_{ij} - i\pi)\coth\beta_{ij} - 1]. \qquad (29)$$

Taking into account the factor of i in going from the energy to the anomalous dimension, Eq. (17), this implies

$$\Gamma = -\frac{\alpha_s}{\pi} \sum_{i<j} \boldsymbol{T}_i \cdot \boldsymbol{T}_j ((\beta_{ij} - i\pi) \coth\beta_{ij} - 1) \quad (30)$$

which agrees exactly with the anomalous dimension extracted from the one-loop calculation, Eq. (8). Thus, we have reproduced *feature 2* in the introduction with a simple classical calculation. Note that with nontrivial color factors, the energy of the state in AdS corresponding to the Wilson line operators becomes a matrix on the space of Wilson lines $\mathcal{W}$ described in Eq. (3). This is a manifestation of the state-operator correspondence in conformal field theory [50].[3]

Before moving on to the other *features*, it is interesting to think about the "wrong" solution, Eq. (20) in AdS. On the sphere, the wrong solution had phantom charges on the antipoles. The location of these phantoms on AdS are shifted from the location of the physical charges by $\beta_{ij}^{\text{phant.}} = \beta_{ij} - i\pi$. That is, the phantom is an initial-state parton pointing in same direction as the outgoing one. So, for example, if we were trying to calculate $e^+ e^- \rightarrow \bar{q}q$, the wrong solution would have corresponded to forward (non) scattering in $\bar{q}q \rightarrow \bar{q}q$, depicted in Fig. 4(b). In contrast to the $e^+ e^- \rightarrow \bar{q}q$, this process has a smooth limit in which the S matrix is just $\mathbb{1}$.

That there is a smooth limit $\gamma \rightarrow 0$ with one incoming and one outgoing Wilson line but not $\beta \rightarrow 0$, with two outgoing or two incoming Wilson lines is closely related to *feature* 3 from the introduction, concerning the complexity of the anomalous dimension. The anomalous dimension is real in DIS, since there is no obstruction to flattening the cusp. In the $e^+ e^- \rightarrow$ dijets case, one cannot remove the cusp for any geodesic separation—the anomalous dimension has an $i\pi$ for any β. For a single log, the $i\pi$ in the anomalous dimension can be seen to come from $\ln(-\frac{\mu^2}{n_i \cdot n_j})$, whose real part is the same as $\ln(\frac{\mu^2}{n_i \cdot n_j})$. For a double log

$$\text{Re}\left[\ln^2\left(-\frac{\mu^2}{n_i \cdot n_j}\right)\right] = \text{Re}\left[\ln^2\left(\frac{\mu^2}{n_i \cdot n_j}\right)\right] - \pi^2. \quad (31)$$

---

[3]In radial quantization, the operators $\mathcal{W}(n_i)$ with different t_{c_i} map to states in the Hilbert space $\mathcal{I}$ with a Hamiltonian given by Eq. (29). One usually considers the state-operator correspondence for local operators, which map to the states on AdS or S^3, depending on the signature. In the presence of Wilson lines in the τ-direction, the Hilbert space changes $\mathcal{H}_{\text{AdS}} \rightarrow \mathcal{H}_{\text{AdS}, \mathcal{W}}$, and we can think of $\mathcal{I}$ in Eq. (4) as the space of lowest-lying states in $\mathcal{H}_{\text{AdS}, \mathcal{W}}$. Interpreting the Wilson lines as infinitely massive charged particles, $\mathcal{I}$ is the space of lowest energy "bound states" of these particles, and the anomalous dimension measures the finite energy differences between different bound states. Additional local operators would map to excitations on top of the states in $\mathcal{I}$.

These π^2 terms get exponentiated leading to large factors of $e^{-\alpha_s \pi^2}$ in cross sections. In fact, this factor is a significant part of the large $\sim$2–3 K-factors in Higgs or Drell-Yan production at the LHC [30,51–54]. Roughly, $\sigma_{\text{NLO}} = \sigma_{\text{LO}} \exp(\gamma_{\text{cusp}}(\alpha_s) C_A \pi^2) \sim 3\sigma_{\text{LO}}$, where the $C_A = 3$ factor comes from these being gg initial states at the LHC, and at leading order $\gamma_{\text{cusp}}(\alpha_s) = \frac{\alpha_s}{\pi} \sim 0.04$. The AdS picture gives us a way to visualize the situations, like DIS, where the anomalous dimension is real and situations like Drell-Yan, where it is complex. Note that, for most processes, the anomalous dimension is a matrix, with some real and some imaginary parts, so this picture is not tremendously useful in general.

Next, we observe that since the Coulomb potential does not get radiative corrections in QED (without propagating fermions), the anomalous dimension derived with energies in AdS is also one-loop exact. This implies that the anomalous dimension of a configuration with two Wilson lines is one-loop exact in QED, which is equivalent to Abelian exponentiation which was *feature 4*. This same reasoning applies to the potential for N charges in QED. This classical proof of Abelian exponentiation is more intuitive than the conventional proof [55] which dissects the relevant Feynman diagrams through repeated use of the eikonal identity and careful consideration of diagrammatic combinatorics.

Beyond Abelian exponentiation, there are results about non-Abelian exponentiation [56,57], including recent generalizations to multijet Wilson lines [58,59]. Non-Abelian exponentiation is not as constraining as Abelian exponentiation, but it does imply that only a reduced set of web diagrams contribute in perturbation theory. There are also intriguing results on the exponentiation properties of Wilson lines for quantum gravity [60–62]. It is natural to expect that there should be a way to understand these results using the AdS language as well, but we leave this for future consideration.

IV. ONE-LOOP RESULTS

For the anomalous dimension at one loop, all that is needed is the classical Coulomb energy between two charges, as calculated in Sec. III. It is helpful to see how this calculation connects directly to the field theory calculation using propagators, which will also set up the discussion of conformal gauge and two-loop results in the next sections. We will perform most of our calculations in the DIS case, where the cusp angle $\gamma = \cosh^{-1}(-n_1 \cdot n_2)$ is real, since that simplifies many of the expressions. We will also use γ in place of β in our AdS coordinates.

The classical Coulomb potential $A_\tau(x)$ can be calculated using the AdS propagator via

$$A_\mu(x) = -i \int d^4 y D_{\mu\nu}(x, y) J^\nu(y) \quad (32)$$

with the current $J^\nu(y)$ of a static charge. Putting the charge at the origin we set $J^\tau(y) = \delta^3(y)$ and $\vec{J}(y) = \vec{0}$, and we have

$$A_\tau(\tau, \gamma) = -i \int_{-\infty}^{\infty} d\tau' D_{\tau\tau}(\tau, \gamma; \tau', 0). \qquad (33)$$

In Minkowski space $\mathbb{R}^{1,3}$ the position-space Feynman propagator is

$$D_{\mu\nu}^F(x, y) = \frac{1}{4\pi^2} \frac{g^{\mu\nu}}{(x-y)^2}. \qquad (34)$$

Projecting onto the τ direction, this becomes

$$D_{\tau\tau}^F(x, y) = D_{\mu\nu}^F(x, y) \frac{\partial x^\mu}{\partial \tau} \frac{\partial y^\nu}{\partial \tau} = \frac{1}{4\pi^2} \frac{x \cdot y}{(x-y)^2}. \qquad (35)$$

Finally, taking $x = e^\tau(-\cosh\gamma, -\sinh\gamma, 0, 0)$ and $y = e^{\tau'}(1, 0, 0, 0)$, we find

$$D_{\tau\tau}^F = -\frac{1}{8\pi^2} \frac{\cosh\gamma}{\cosh(\tau - \tau') + \cosh\gamma}, \qquad (36)$$

so that

$$A_\tau(\tau, \gamma) = -i \int_{-\infty}^{\infty} d\tau' D_{\tau\tau}^F = \frac{i}{4\pi^2} \gamma \coth\gamma. \qquad (37)$$

This is the same result we found in the previous section Eq. (28), up to an undetermined additive constant. We can again fix the constant by specifying which energy we mean by matching to the case of a conserved current with $\gamma = 0$, to get $\gamma \coth\gamma - 1$.

The propagator calculation lets us connect the energy directly to the anomalous dimension. Consider the one-loop calculation with the gluon exchanged between the two Wilson lines. In position space, the integral is

$$I = \frac{g^2}{(4\pi)^2} \int_\infty^0 ds \int_0^\infty dt \frac{n_1 \cdot n_2}{(sn_1 - tn_2)^2}. \qquad (38)$$

Pulling out the overall scale and changing to radial coordinates via $t = se^\tau$ this becomes

$$I = \frac{g^2}{2(4\pi)^2} \int_0^\infty \frac{ds}{s} \int_{-\infty}^\infty d\tau \frac{\cosh\gamma}{\cosh\tau + \cosh\gamma}, \qquad (39)$$

where we have used $\cosh\gamma = -n_1 \cdot n_2$ as usual. The first integral is scaleless, resulting from the fact that our configuration of Wilson lines is rescaling-invariant. In general, one must break rescaling invariance with UV and IR regulators, and carefully extract the coefficients of the UV divergences to compute the anomalous dimension. However at one loop, we can be more cavalier. With regulators in place $\int \frac{ds}{s}$ will become $\log\frac{\Lambda_{\rm UV}}{\Lambda_{\rm IR}}$, so that the one-loop anomalous dimension is simply the coefficient of this scaleless integral. This is precisely Eq. (29), the energy

of the charges in AdS, as expected. In the field theory calculation the -1 factor that appears in the energy is correctly reproduced by the self-energy graphs for $n_i^2 \neq 0$. This calculation makes the connection transparent at the level of the integrals.

V. LIGHTLIKE LIMIT

In this section, we consider the lightlike limit $n_i^2 \to 0$ which was the subject of *feature* 5. In this limit the static sources on the AdS space (corresponding to the Wilson lines) move towards the boundary of AdS, $\gamma_{ij} \to \infty$ or $\beta_{ij} \to \infty$. The anomalous dimension becomes linear in the cusp angles, which diverge as $\beta_{ij} \to \infty$ or $\gamma_{ij} \to \infty$. Equivalently, the imaginary part of the energy becomes linear in the geodesic distance between the charges, while the real part goes to a constant [see Eq. (28)]. This is a qualitatively very different behavior from flat space, where the energy vanishes as the inverse of the distance.

If we try to actually set $n_i^2 = 0$, the cusp angle is infinite and the energy is formally infinite, indicating new unregulated singularities. The linearly diverging cusp angle is connected to the appearance of additional collinear divergences that appear in both the ultraviolet and infrared in the anomalous dimension computation. Effectively in the computation of matrix elements of $\mathcal{W}$ we are forced to introduce a small dimensionful IR regulator Λ. With UV divergences regulated in dimensional regularization the dimensions are compensated by μ, so $1/|n| \to \Lambda/\mu$, giving the form in Eq. (11). Introducing Λ/μ is equivalent to moving lightlike charges away from the boundary of AdS, so that we can still sensibly talk about the geodesic distance between charges. The dependence on the IR regulator cancels out in physical cross section computations. For example, eikonal scattering involves a square of $\mathcal{W}$ matrix elements which yields the soft function $S(k)$ in Eq. (6). In this case the IR divergences cancel between virtual and real emission diagrams and Λ is replaced by the observed momenta of particles, $\Lambda \to k$.

To secure a clearer physical picture of what this growing imaginary energy means, consider the case of two outgoing lightlike partons, such as in dijet production. In Fig. 5, we contrast the electric field of a normal pair of charges, in flat space, with the imaginary part of the electric field for two charges in AdS. As the total energy grows with separation, the electric field approaches a constant between the charges. Notice that in the presence of two opposite Abelian charges, $\text{Im}(E)$ is always negative, as should be the case for the energy of an unstable state. Back in Minkowski space, this corresponds to a roughly constant density of radiation between the two charges. The third panel of Fig. 5 shows this behavior in a Monte Carlo simulation [63]. To generate this distribution, a 200 GeV dijet event produced at 7 TeV center of mass energy at the LHC was simulated. The figure shows the accumulated energy distribution. Note that the radiation is concentrated
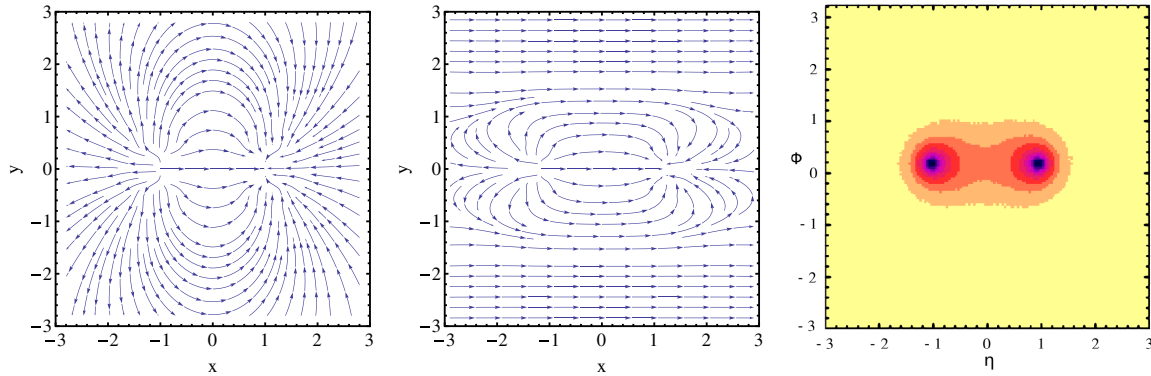
FIG. 5 (color online).   On the left are the electric field lines for two charges in flat space. The middle shows the imaginary part of the electric field for two charges in AdS, after projecting to rectangular coordinates with $x = \beta \sin\theta$ and $y = \beta \cos\theta$. The right (from [87]), shows the distribution of radiation from a color singlet scalar decaying to two jets at the LHC. The axes in this case are pseudorapidity and azimuthal angle, and the contours correspond to factors of two in the accumulated energy distribution. The rightmost plot is included to remind the reader that a color dipole radiates between the color charges, which roughly corresponds to the region where the energy density has support in the AdS picture. The sharp dropoff of the radiation pattern in the effect of color coherence. In a qualitative sense only, this corresponds to the exponential decay of the radiation away from the dipole axis in the AdS picture.

between the two charges, and suppressed away from the dipole axis, just as the energy distribution is in AdS.

Linear growth of energy with separation is normally an indication of confining behavior. In this case, since the energy is imaginary, it is not confinement in the usual sense, but can still be interpreted as a type of confinement. In a sense, this linear growth of the (imaginary) energy with separation is related to the fact that high-energy quarks always appear with an accompanying jet, whose dynamics are described with Sudakov factors. Although this "Sudakov confinement" of quarks inside jets has little in common with confinement in QCD, it is not an unreasonable phrase for the linearly growing energy in AdS.

To be specific, consider the case of one incoming and one outgoing Wilson line, as in deep inelastic scattering (DIS). In DIS, an electron is scattered off of a proton, with Bjorken x defined in terms of the momentum transfer q^μ and the proton momentum P^μ as $x = -q^2/2P \cdot q$. In the $x \to 1$ limit of DIS at large $Q^2 = -q^2$, the outgoing radiation becomes jetlike, with its mass $m_J^2 = Q^2(1-x)/x$ getting small. In this limit, the Wilson line description applies and important physics is encoded in the anomalous dimension. We saw that when Wilson lines becomes light-like, the cusp angle $\gamma_{12} \to \infty$ and the energy in AdS becomes

$$E_{\text{tot}} \to i\frac{\alpha_s}{\pi}\gamma_{12} \tag{40}$$

which is an imaginary energy.

An imaginary energy is indicative of nonunitary time evolution. Since time in AdS is scale in Minkowski space, this is nonunitary evolution as the scale is changed. One way to think of the violation of unitary is going from a simple state, with say a single quark, to a state with a quark

and a gluon. The probability for this to happen is given by the Alterelli-Parisi splitting kernels. The quark-gluon splitting kernel is

$$P_{q \to qg}(z, p_T) = \frac{\alpha_s}{\pi}\frac{1+z^2}{1-z}\frac{1}{p_T}, \tag{41}$$

where z is the fraction of energy in the quark, which must be close to 1 (the Wilson line picture only applies in the $x \to 1$ limit) and p_T is the transverse momentum of the gluon with respect to the quark direction. The integral over this splitting function is infrared-divergent. Typically, one imagines the quark starts off at a scale $\mu \sim Q$ characteristic of the hard scattering; then it evolves down to a scale $\mu \sim p_T$ [17,18]. The probability of not having emitted a gluon between these scales is

$$\Sigma(Q, p_T) = \exp\left(-\int_{p_T}^{Q} d\mu \int_{Q/\mu}^{1} dz P(1-z, \mu)\right)$$
$$= \exp\left(-\frac{\alpha_s}{\pi}\ln^2\frac{Q}{p_T} + \dots\right). \tag{42}$$

This quantity is known as a Sudakov factor. It is a no-branching probability, and used as a classical probability in Monte Carlo event generators, which treat the parton as showering off gluons through a Markov process, see for example [63]. The rate of emission is exactly proportional to the coefficient of linear growth of the energy in AdS, a quantity known as the *cusp-anomalous dimension*.

So we see that the nonunitary evolution corresponds to the probability that an off-shell quark decays into a gluon and a slightly less off-shell quark. The constant energy density in AdS at large cusp angle corresponds to a constant probability for emission per unit scale. If we evaluate the Sudakov factor at $p_T = 0$, we see that there is zero

probability for a quark to evolve forever without emitting a gluon. In physical situations, there is always a finite IR cutoff, such as the hadronization scale Λ_{QCD} or a resolution scale for the jet. Nevertheless, at late times in AdS, or small momentum scales in Minkowski space, the original state approaches zero amplitude. Thus, there is no probability that we will find a free quark at asymptotically late times when produced at a finite scale Q. In other words, there are no free quarks which are not confined within jets. In fact, the characteristic size of a jet is precisely determined by the cusp-anomalous dimension in the Sudakov factor.

It would be interesting to further explore the analogy between confinement and the linear growth of (imaginary) energy with distance. For example, one might argue that the energy can grow at most linearly with separation [64], as expected from the string flux tube picture. The analogy would connect this directly to Sudakov confinement and the linear dependence of the anomalous dimensions on $\log\mu$ for various fields in scattering processes. Then, perhaps, by reversing the logic, the Sudakov factors could give insight to confining gauge theories from the study of jets.

VI. CONFORMAL GAUGES

We have seen that radial quantization is a useful picture for understanding the one-loop cusp-anomalous dimension. In $\mathbb{R} \times \mathrm{AdS}$, a cusp maps to a collection of charges, and $\Gamma_{\mathrm{cusp}}^{1-\mathrm{loop}}$ has an interpretation in terms of static potentials. It makes sense that for higher-loop computations, we should keep the separation between the τ direction and the AdS directions manifest. However, this is not done in typical calculations. The reason is that although the action S_{YM} is conformally invariant, the *gauge-fixing terms* are not. For example, in Feynman gauge, we have

$$S = S_{\mathrm{YM}} + S_{\mathrm{g.f.}},$$
$$S_{\mathrm{g.f.}} = \int d^4 x \sqrt{-g}\, \frac{1}{2}(\nabla^\mu A_\mu)^2 + S_{\mathrm{ghost}}. \qquad (43)$$

Under a conformal rescaling $g_{\mu\nu} = e^{2\omega} g'_{\mu\nu}$, the covariant derivative transforms nontrivially,

$$\sqrt{-g}(\nabla^\mu A_\mu)^2 = \sqrt{-g'}(\nabla'^\mu A_\mu + 2\partial^\mu \omega A_\mu)^2. \qquad (44)$$

Consequently, a gauge that appears natural in one conformal frame may look somewhat unnatural in another. For instance, a useful feature of Feynman gauge in flat Minkowski space is that the propagator does not mix different polarizations between different points: $\varepsilon^\mu \Pi_{\mu\nu} \propto \varepsilon_\nu$. However from the point of view of radial coordinates $(\tau, \beta, \theta, \phi)$, the Feynman-gauge propagator transports polarizations from one point to another in a nontrivial way. More precisely, transport via the propagator is not proportional to parallel transport in the $\mathbb{R} \times \mathrm{AdS}$ metric. This is clear from the transformation law (44): plugging in $g_{\mathbb{R}^{1,3}} = e^{2\tau} g_{\mathbb{R} \times \mathrm{AdS}}$, we see that $S_{\mathrm{g.f.}}$ includes kinetic mixing

between A_τ and the spatial components A_i. Throughout this section, we will use $i = 1, 2, 3$ to denote the directions in AdS.

It is informative to look at the explicit form of the mixing. To decompose the propagator, first observe that the τ component of the propagator comes from projections onto $\frac{\partial x^\mu}{\partial \tau} = x^\mu$. So that $D_{\tau\nu} = x^\mu D_{\mu\nu}$. Thus we can decompose the polarization $g^{\mu\nu}$ in the numerator of the Feynman propagator as

$$g^{\mu\nu} = [g^{\mu\nu} - \hat{x}^\mu \hat{x}^\nu - \hat{y}^\mu \hat{y}^\nu + (\hat{x} \cdot \hat{y})\hat{x}^\mu \hat{y}^\nu]$$
$$+ [(\hat{x} \cdot \hat{y})\hat{x}^\mu \hat{y}^\nu] + [\hat{x}^\mu \hat{x}^\nu + \hat{y}^\mu \hat{y}^\nu - 2(\hat{x} \cdot \hat{y})\hat{x}^\mu \hat{y}^\nu], \qquad (45)$$

where $\hat{x} = x^\mu/|x|$ and $\hat{y} = y^\mu/|y|$. The first term in brackets vanishes when contracted with x^μ or y^ν, so it represents the spatial components of the Feynman-gauge propagator from the point of view of AdS, i.e. D_{ij}. This can also be seen by writing it as

$$g^{\mu\nu} - \hat{x}^\mu \hat{x}^\nu - \hat{y}^\mu \hat{y}^\nu + (\hat{x} \cdot \hat{y})\hat{x}^\mu \hat{y}^\nu$$
$$= |x||y| \frac{\partial}{\partial x_\mu} \frac{\partial}{\partial y_\nu}\left(\frac{x \cdot y}{|x||y|}\right), \qquad (46)$$

which vanishes when contracted with x_μ or y_ν since the dilation operator $\mathcal{D} = x^\mu \partial_\mu$ automatically annihilates any scale-invariant function. The second term in Eq. (45) is $D_{\tau\tau}$, as in Eq. (36). The third term represents the nonzero $D_{\tau i}$ and $D_{i\tau}$ mixing present in Feynman gauge.

Since the Wilson lines only source A_τ, at one loop only the $D_{\tau\tau}$ component of the propagator contributes. If we try to use the same propagator in higher-loop computations, even though the Wilson lines only source A_τ, due to the $D_{\tau i}$ mixing terms, there will be interactions involving $(A_i)^3$ vertices which make the calculations complicated. However, we have seen that anomalous dimensions of Wilson lines are most naturally thought about from the point of view of $\mathbb{R} \times \mathrm{AdS}$. In a gauge more suited to this space there should be no mixing, and A_τ can be treated as a charged scalar. Since there is no scalar cubic or quartic vertex $(A_\tau)^{3,4}$ in Yang-Mills theory, the calculation will be significantly simpler. Vertices $(A_i)^2 A_\tau$ remain active when we consider Wilson line operators in this gauge and enter for the leading vacuum polarization effects.

We will refer to gauges with the property that A_τ and A_i do not mix as *conformal gauges*, to emphasize the fact that they are most natural in a different conformal frame from the usual one. This nonmixing is not an overly restrictive condition and there are many gauges that satisfy it (for example, the condition remains true after any τ-independent gauge transformation). Perhaps the simplest example of a conformal gauge is temporal gauge in $\mathbb{R} \times \mathrm{AdS}$, or equivalently "radial gauge" in $\mathbb{R}^{1,3}$, in which $A_\tau = x^\mu A_\mu = 0$ and radial Wilson lines are actually trivial. We will briefly discuss this gauge in Sec. VIB. In

Sec. VI A we will focus on a less singular example of conformal gauge, which corresponds to a quantum average over different gauge conditions, as in R_ξ gauges.

A. Derivation of Conformal Gauge in d dimensions

To arrive at a conformal gauge, perhaps the most familiar strategy would be to study gauge-fixing terms in $\mathbb{R} \times$ AdS, and then invert the kinetic terms to form the corresponding propagators. This might be an interesting exercise, but it would be needlessly complicated for our purposes. Instead, we will adopt the more pragmatic procedure of directly gauge-transforming the Feynman-gauge propagator and solving for the transformation function that gives the desired properties. This then implicitly specifies Becchi-Rouet-Stora-Tyutin exact gauge-fixing terms, including a ghost action.

Our goal is to derive a gauge that has no τ-i mixing in d dimensions that is suitable for use in dimensional regularization. Our procedure is simple, and powerful enough to handle this even though Yang-Mills theory is only classically conformally invariant when $d = 4$. Instead of sorting out details of conformal anomalies at order ε, we will keep the d-dimensional Minkowski metric and flat coordinates x_μ, and simply search for a gauge that respects the foliation of $\mathbb{R}^{1,d-1}$ into $\mathbb{R} \times$ AdS$_{d-1}$. Precisely when $d = 4$, our propagator will have an interpretation as the propagator in a gauge theory on $\mathbb{R} \times$ AdS$_3$. However when ε is nonzero, it will simply be a useful tool that enables computations to be performed without encountering mixing terms $D_{\tau i}$ or $D_{i\tau}$ in d dimensions.

We begin with the position-space Feynman propagator in d dimensions

$$D^F_{\mu\nu}(x, y) = -g_{\mu\nu} \frac{\kappa_d}{[-(x - y)^2 + i\epsilon]^{d/2-1}}, \qquad (47)$$

where $\kappa_d = \frac{\Gamma(d/2-1)}{4\pi^{d/2}}$ is a constant. Since the propagator depends only on quadratic terms in the action, it is sufficient for our discussion here to consider an Abelian theory. In a non-Abelian theory, the propagator should also include a factor of the identity δ^{ab} in color space, and we have the additional Feynman rules involving ghosts which we discuss in Appendix B.

We will consider a class of propagators given by

$$D_{\mu\nu}(x, y) = D^F_{\mu\nu}(x, y) + \frac{\partial}{\partial y^\nu} \Lambda_\mu(y, x) + \frac{\partial}{\partial x^\mu} \Lambda_\nu(x, y), \qquad (48)$$

where $\Lambda_\mu(y, x)$ is a one-form at x, depending on both x and y. Notice that $D_{\mu\nu}$ is still an inverse for the kinetic term in the space of gauge equivalence classes, though it differs from $D^F_{\mu\nu}$ along gauge orbits. Indeed, suppose J^μ is a conserved current, and consider the associated vector potential

$$A_\mu(x) \equiv -i \int dy D_{\mu\nu}(x, y) J^\nu(y)$$

$$= -i \int dy D^F_{\mu\nu}(x, y) J^\nu(y) + \frac{\partial}{\partial x^\mu}$$

$$\times \left(-i \int dy \Lambda_\nu(x, y) J^\nu(y) \right)$$

$$= A^F_\mu(x) + \partial_\mu \left(-i \int dy \Lambda_\nu(x, y) J^\nu(y) \right), \qquad (49)$$

where we have integrated by parts and used current conservation. Since A_μ differs from A^F_μ only by a gauge transformation, it still solves Maxwell's equation $\partial_\mu F^{\mu\nu} = J^\nu$.

We would like $D_{\tau i}$ to vanish, so that the propagator does not mix time and space directions in $\mathbb{R} \times$ AdS. Recalling that τ is the generator of scale transformations, $\partial_\tau = x^\mu \partial_\mu$, a vector field $A_\mu(y)$ will have no τ component if $y^\mu A_\mu(y) = 0$. Thus our condition is

$$x^\mu D_{\mu\nu}(x, y) A^\nu(y) = 0 \quad \text{whenever} \quad y_\nu A^\nu(y) = 0. \qquad (50)$$

Likewise, for $D_{i\tau}$ to vanish we have the condition $A^\mu(x) D_{\mu\nu}(x, y) y^\nu = 0$ whenever $x_\mu A^\mu(x) = 0$. Note that Eq. (50) is not translation-invariant, it treats the origin as a special point and yields propagators that are not simply functions of $x - y$.[4] The general class of conformal gauges which satisfy these no-mixing conditions is derived in Appendix A. Here let us consider the ansatz

$$\Lambda_\mu(y, x) = \kappa_d \frac{x_\mu}{|x|^{d-2}} g(\alpha, \beta), \quad \text{where} \quad \alpha \equiv \frac{x \cdot y}{|x||y|},$$

$$\beta \equiv \frac{|y|}{|x|}, \qquad (51)$$

and $g(\alpha, \beta)$ is some function to be determined. Equation (50) implies

$$\frac{\partial}{\partial \alpha} g(\alpha, \beta) = \beta(2\alpha\beta - \beta^2 - 1)^{1-d/2}$$

$$g(\alpha, \beta) = \frac{1}{4 - d}[(2\alpha\beta - \beta^2 - 1)^{2-d/2} - f(\beta)^{2-d/2}], \qquad (52)$$

where $f(\beta)$ is arbitrary and its $2 - d/2$ power produces the correct $d \to 4$ solution. Our ansatz becomes

$$\Lambda_\mu(y, x) = \frac{\kappa_d}{4 - d} \frac{x_\mu}{x^2} \{[-(x - y)^2]^{2-d/2} - |x|^{4-d} f(\beta)^{2-d/2}\}. \qquad (53)$$

---

[4] In our setup the origin is special since it is the location of our hard interaction and the place where cusps occur between Wilson lines. This explains why it is useful to consider non-translationally invariant gauges, even though the final physical results are gauge independent and translationally invariant.

The conformal gauge propagator is then

$$D_{\mu\nu}(x, y) = -\frac{\kappa_d}{[-(x-y)^2]^{d/2-1}}\left(g_{\mu\nu} - \frac{x_\mu x_\nu}{x^2} - \frac{y_\mu y_\nu}{y^2}\right.$$
$$\left. + \frac{2x_\mu(x\cdot y)y_\nu}{x^2 y^2}\right) + \kappa_d \frac{x_\mu y_\nu}{x^2 y^2}\{[-(x-y)^2]^{2-d/2}$$
$$- \chi(|x|, |y|)^{4-d}\}, \qquad (54)$$

where $\chi(|x|, |y|)$ is any symmetric function of $|x|$ and $|y|$ with dimensions of length. [χ has a a simple but unenlightening relation to $f(\beta)$]. Separating out the τ and spatial components, as in Eq. (45), this can be written

$$D_{\mu\nu}(x, y) = -\frac{\kappa_d}{[-(x-y)^2]^{d/2-1}}|x||y|\partial_\mu^x \partial_\nu^y\left(\frac{x\cdot y}{|x||y|}\right)$$
$$- \kappa_d \frac{x_\mu y_\nu}{x^2 y^2}\left(\frac{x\cdot y}{[-(x-y)^2]^{d/2-1}}\right.$$
$$\left. - [-(x-y)^2]^{2-d/2} + \chi(|x|, |y|)^{4-d}\right). \qquad (55)$$

Here the first term is manifestly "angular," involving derivatives acting on a scaleless quantity which vanish when contracted with x^μ or y^ν, as in Eq. (46). The second term is "radial," involving projection onto the τ-direction with x_μ and y_ν. The mixing terms have been gauged away, as desired.

A natural choice is to take χ to be d-independent. Then when $d = 4$ the last two terms of Eq. (55) cancel, χ drops out, and we have a unique 4D propagator. In fact, this propagator is identical to the Feynman propagator in 4D, Eq. (36), without the mixing terms. In particular, the calculation of the Coulomb potential from a static charge in AdS, and hence the one-loop anomalous dimension of the Wilson line, is identical in Feynman gauge and in conformal gauge. We see that the entire content of this gauge fixing is to move the mixing terms in Feynman gauge into nonmixing terms starting at order ε.

Equation (55) is convenient for computations involving non-lightlike Wilson lines in d dimensions or with dimensional regularization. To consider propagation between points on two lightlike Wilson lines we take $x^\mu = \lambda_1 n_1^\mu$ and $y^\mu = \lambda_2 n_2^\mu$, and take the limit $n_1^2 \to 0$ and $n_2^2 \to 0$. Here $n_1^\mu n_2^\nu D_{\mu\nu}(x, y)$ reduces to the same result as Feynman gauge in 4D. In d dimensions the result in Eq. (55) is not convenient because the χ term does not scale in the same manner as the other terms in the radial part of the propagator. We derive an alternative conformal gauge with a good scaling limit for lightlike Wilson lines in d dimensions in Appendix A.

B. Comparison to radial gauge

In conformal gauge, the scalar modes in AdS, A_τ which are produced from the Wilson lines, have no mixing with the vector modes. This simplifies some loop calculations, as we will demonstrate in the next section. However, it is natural to ask why we cannot simplify things even further by choosing temporal gauge $A_\tau = 0$ in AdS. This condition becomes $x_\mu A^\mu(x) = 0$ in Minkowski space, and gauges satisfying it are called radial (or Fock-Schwinger) gauges. The origin is again a special point for these gauges and the gauge-boson propagator is not translation-invariant.

In radial gauge, our N-jet Wilson lines become trivial, and loop corrections to the expectation value $\langle \mathcal{W} \rangle$, and corresponding anomalous dimension, seem naively to vanish. Of course this is too simplistic to be correct. The problem is that an N-jet Wilson line operator $\mathcal{W}$ as defined in Eq. (3) is only invariant by itself under gauge transformations which vanish at infinity. However, the transformation from, say, Feynman gauge to radial gauge is nontrivial at infinity, so the expectation value $\langle \mathcal{W} \rangle$ can change. Indeed, in Ref. [65] it was shown that the radial gauge propagator $D_{\mu\nu}$ itself carries ultraviolet divergences.

To correctly compute the cusp-anomalous dimension, we must either restrict ourselves to gauges with appropriate behavior at spatial infinity, or "close off" our Wilson loop in a gauge-invariant way at some large finite distance from the origin, without introducing additional cusps. (Or with additional cusps whose contribution we then subtract away.) In the latter case, the cusp divergences are generated by a different part of the calculation. For example, using a conventional definition of radial gauge, Ref. [65] explicitly demonstrates that the classic one-loop $x = 0$ cusp-anomalous dimension is correctly reproduced by the (smooth) "closed-off" part of the Wilson loop. The fact that the radial gauge propagator itself is ultraviolet-divergent plays a crucial role in this computation, since otherwise the closed-off part of the loop would not contribute to the anomalous dimension.

To avoid having these complications, we will focus on conformal gauges that do not have ultraviolet divergences in $D_{\mu\nu}$. This was true of our construction in Sec. VI A, where $D_{\mu\nu}$ in Eq. (55) is finite as $d \to 4$, and divergences occur only when interaction points approach each other. In the limit $(x - y)^2 \to 0$, with both x^2, $y^2 \neq 0$, $D_{\mu\nu}$ approaches the usual Feynman propagator at leading order. Consequently, power counting shows that divergences originating near points away from the light cone are identical in Feynman gauge and in our conformal gauge. (It would be useful to fully characterize the divergence and subdivergence structure of multiloop diagrams in conformal gauge.) In these cases, the cusp-anomalous dimension can be computed by considering only a neighborhood of the cusp.

VII. THREE WILSON LINES AT TWO LOOPS

As a concrete application of using our conformal gauge, let us compute the two-loop contribution to the anomalous dimension of a multi-Wilson line operator Eq. (3) that
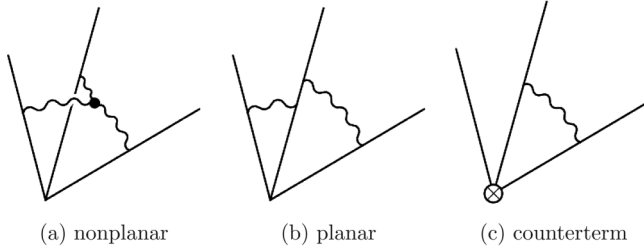
FIG. 6. Two-loop graphs contributing to the coefficient $F(\gamma_{ij}, \gamma_{jk}, \gamma_{ki})$ of the antisymmetric color structure in $\Gamma_{\text{cusp}}(v_i)$ (Eq. (56)).

involves all three lines. The absence of τ-i mixing makes this computation extremely simple, and elucidates the origin of the previously mysterious pairwise structure of the result, discussed as *feature 6*.

When the number N of jet directions is three or more, the anomalous dimension $\Gamma_{\text{cusp}}(n_i)$ can in principle depend on arbitrary combinations of the cusp angles γ_{ij}. Nontrivial combinations involving three γ_{ij}'s can appear first at two loops in the coefficient F of the "maximally non-Abelian" color structure $f^{abc}\boldsymbol{T}_i^a\boldsymbol{T}_j^b\boldsymbol{T}_k^c$,

$$\Gamma_{\text{cusp}}^{2-\text{loops}}(n_i) = \left(\frac{\alpha_s}{\pi}\right)^2 \left(\sum_{i<j} \boldsymbol{T}_i^a \boldsymbol{T}_j^a f(\gamma_{ij})\right.$$
$$\left. + \sum_{i<j<k} if^{abc}\boldsymbol{T}_i^a\boldsymbol{T}_j^b\boldsymbol{T}_k^c F(\gamma_{ij}, \gamma_{jk}, \gamma_{ki})\right),$$
(56)

due to the presence of diagrams depicted in Fig. 6. In particular the nonplanar diagram 6(a) could naïvely contribute a complicated function of all three cusp angles. The expression for this graph in Feynman gauge was discussed in the lightlike limit in [37,66], and analyzed numerically in [67]. It was finally computed for general cusp angles in [68] in a somewhat technical computation using Mellin-Barnes representations. After all this, the final result turns out to be remarkably simple,

$$F_{\text{Feyn.}}^{(a)} = -\frac{1}{2}(\gamma_{ij} \coth\gamma_{ij})\gamma_{jk}^2 + \text{antisym.} \quad (57)$$

where "antisym." stands for signed permutations of i, j, k. This is a sum of terms each of which only depends on two of the cusp angles.

It is less surprising that the planar and counterterm graphs also have a pairwise form. For the antisymmetric color structure, the result is [68]

$$F_{\text{Feyn.}}^{(b)} + F_{\text{Feyn.}}^{(c)} = \frac{1}{2}(\gamma_{ij} \coth\gamma_{ij}) \times \coth\gamma_{jk}$$
$$\times \left(\gamma_{jk}^2 + 2\gamma_{jk}\log(1 - e^{-2\gamma_{jk}})\right.$$
$$\left. - \text{Li}_2(e^{-2\gamma_{jk}}) + \frac{\pi^2}{6}\right) + \text{antisym.} \quad (58)$$

When all the Wilson lines are lightlike, the sum of graphs actually vanishes in Feynman gauge, a result which is not immediately obvious. At large γ, the $-\frac{1}{2}\gamma_{ij}\gamma_{jk}^2$ asymptotic behavior of the nonplanar amplitude in Eq. (57) is exactly canceled by contributions from Eq. (58).

Returning to the difficult nonplanar graph, the simplicity of the final result $F_{\text{Feyn}}^{(a)}$ is easily understood from the AdS picture. In $\mathbb{R} \times \text{AdS}$, each Wilson line points in the time direction, and thus sources only the τ component of the gauge field. In conformal gauge A_τ does not mix with A_i, then the interaction vertex in 6(a) involves three τ-polarized gauge fields, and thus vanishes identically. In this gauge, only the planar and counterterm diagrams contribute, and F naturally has a pairwise-factorized form. Note that one of the factors ($\gamma_{ji}\coth\gamma_{ij}$) looks just like $\Gamma_{\text{cusp}}^{1-\text{loop}}$. This is suggestive that the contribution of $F_{\text{Feyn}}^{(a)}$ should come from the counterterm graph in conformal gauge. We will shortly show that this is indeed the case.

Let us rephrase the above argument in a way that emphasizes the analogy with our one-loop computation in Sec. III. Notice that each line in 6(a), thought of as a static charge in AdS, couples only to the τ-independent modes of the gauge field in $\mathbb{R} \times \text{AdS}$.[5] Thus, the computation of this graph "dimensionally reduces" from $\mathbb{R} \times \text{AdS}$ to AdS, with one overall τ-integral contributing a logarithmic divergence multiplying the anomalous dimension. The theory on AdS contains a scalar (coming from A_τ), and a three-dimensional gauge field. Each Wilson line sources the scalar, so Fig. 6(a) becomes a three-point function of scalars in AdS. Finally, since there is no three-scalar interaction in the dimensional reduction of Yang-Mills theory, this correlator vanishes at leading order. The utility of conformal gauge is that it makes dimensional reduction in the τ-direction much simpler than it would be in Feynman gauge.

Having understood why $F(\gamma_{ij}, \gamma_{jk}, \gamma_{ki})$ should have a simple form, let us proceed to compute it using conformal gauge. Figure 6(a) now vanishes, and the entire contribution comes from the planar and counterterm graphs. All Wilson lines point in the τ-direction, so we need only the radial part of the gauge-boson propagator which from Eq. (55) is

$$D_{\mu\nu}^{(\tau\tau)}(x, y) = -\kappa_d \frac{x_\mu y_\nu}{x^2 y^2}\left(\frac{x \cdot y}{[-(x-y)^2]^{d/2-1}}\right.$$
$$\left. - [-(x-y)^2]^{2-d/2} + \chi(|x|, |y|)^{4-d}\right). \quad (59)$$

The first term in parentheses is the same as $D_{\tau\tau}^F$ in Feynman gauge. The second and third terms are new.

---

[5]This is not the case for diagrams involving more than one gluon emission from a single Wilson line.

Since we seek the coefficient of the antisymmetric color structure $f^{abc}T_i^a T_j^b T_k^c$, which does not arise at one loop, the anomalous dimension is simply the coefficient of the $1/\varepsilon$ pole in the sum of diagrams 6(b) and 6(c). To separate UV and IR divergences, we must in general regulate the IR with something other than dimensional regularization. However, here we can safely ignore this subtlety since the entire divergence structure comes from a single scaleless integral, and it will be simple to isolate the associated UV divergence. We have checked that a more careful treatment of the infrared, for instance giving the Wilson lines some finite length, yields the same results.

To evaluate 6(b), let us first perform the integrals along the lines with only a single gluon emission. This gives the Coulomb potential from a single Wilson line, which we now need up to order ε. We have, with the normalization $n_1^2 = n_2^2 = 1$,

$$
\int_0^\infty ds n_i^\mu n_j^\nu D_{\mu\nu}(sn_i, tn_j)
$$

$$
= \kappa_d(-1)^\epsilon \int_0^\infty ds\left(\frac{-n_i \cdot n_j}{(sn_i - tn_j)^{2-2\epsilon}}\right.
$$

$$
\left. + \frac{\chi(s,t)^{2\epsilon} - (sn_i - tn_j)^{2\epsilon}}{st}\right)
$$

$$
= \kappa_d \frac{(-1)^\epsilon}{t^{1-2\epsilon}}(E_F^{(0)}(\gamma_{ij}) + \varepsilon E_F^{(1)}(\gamma_{ij}) + \varepsilon E_C^{(1)}(\gamma_{ij})). \quad (60)
$$

Here $E_F^{(0)} = A_\tau(\gamma_{ij})$ from Eq. (37) is just the scalar potential from a Wilson line in four dimensions

$$
E_F^{(0)}(\gamma) = \gamma \coth\gamma. \quad (61)
$$

$E_F^{(1)}$ is the next term in the ε expansion of this potential in Feynman gauge, also coming from the first term in the integral. It is

$$
E_F^{(1)}(\gamma) = \coth\gamma\left(\gamma^2 + 2\gamma \log(1 - e^{-2\gamma})\right.
$$

$$
\left. - \text{Li}_2(e^{-2\gamma}) + \frac{\pi^2}{6}\right). \quad (62)
$$

Finally, $E_C^{(1)}$ is the new piece present in conformal gauge and not in Feynman gauge, from the second term in the integral in Eq. (60). It gives

$$
E_C^{(1)}(\gamma_{ij}) = \int_0^\infty \frac{ds}{s} \log\frac{\chi(s,1)^2}{(n_i s - n_j)^2}
$$

$$
= \int_{-\infty}^\infty d\tau \log\left(\frac{\cosh\tau}{\cosh\tau + \cosh\gamma_{ij}}\right)
$$

$$
+ \int_0^\infty \frac{ds}{s} \log\frac{\chi(s,1)^2}{1 + s^2}
$$

$$
= -\gamma_{ij}^2 - \frac{\pi^2}{4} + c_\chi. \quad (63)
$$

The constant c_χ is a gauge-dependent but γ-independent number which will cancel from the final result (and is exactly zero for $\chi(|x|, |y|) = \sqrt{x^2 + y^2}$). Note that the asymptotic expansion of $E_C^{(1)}$ at large γ is $-\gamma^2$, which cancels the asymptotic expansion of $E_F^{(1)}$, leaving zero contribution to the antisymmetric color structure in the anomalous dimension for the lightlike limit. Two-loop graphs involving only two lines do contribute in the lightlike limit, and give an energy which grows linearly with the cusp angle.

With $\mathcal{O}(\varepsilon)$ parts of the scalar potential calculated, it is now easy to extract the antisymmetric part of the two-loop anomalous dimension. The counterterm and planar graphs can be combined into

$$
I^{(b)} + I^{(c)} = \int_0^\infty \frac{dt_1}{t_1^{1-2\varepsilon}}[E_F^{(0)}(\gamma_{ij}) + \varepsilon E_F^{(1)}(\gamma_{ij})
$$

$$
+ \varepsilon E_C^{(1)}(\gamma_{ij})]\left\{-\frac{1}{\varepsilon}E_F^{(0)}(\gamma_{jk})\right.
$$

$$
+ \int_0^{t_1} \frac{dt_2}{t_2^{1-2\varepsilon}}[E_F^{(0)}(\gamma_{jk}) + \varepsilon E_F^{(1)}(\gamma_{jk})
$$

$$
\left. + \varepsilon E_C^{(1)}(\gamma_{jk})]\right\} + \text{antisym.} \quad (64)
$$

After antisymmetrizing, everything vanishes except for the cross term between the counterterm and the ε terms on the first line. Replacing the scaleless t_1 integral on the first line with $\frac{1}{2\varepsilon}$ as before, we see that these graphs sum to produce a contribution to the anomalous dimension of the form

$$
F^{(b)} + F^{(c)} = \frac{1}{2}E_F^{(0)}(\gamma_{ij})(E_F^{(1)}(\gamma_{jk}) + E_C^{(1)}(\gamma_{jk}))
$$

$$
+ \text{antisym.},
$$

$$
= \frac{1}{2}\gamma_{ij}\coth\gamma_{ij}\coth\gamma_{jk}\left(\gamma_{jk}^2 + 2\gamma_{jk}\log(1 - e^{-2\gamma_{jk}})\right.
$$

$$
\left. - \text{Li}_2(e^{-2\gamma_{jk}}) + \frac{\pi^2}{6}\right) - \frac{1}{2}\gamma_{ij}\coth\gamma_{ij}\gamma_{jk}^2
$$

$$
+ \text{antisym.} \quad (65)
$$

which precisely matches $F^{(a)} + F^{(b)} + F^{(c)}$ in Feynman gauge. The difficult nonplanar graph was reproduced with a far simpler calculation involving the $\mathcal{O}(\varepsilon)$ parts of the conformal gauge propagator. Note that the gauge-dependent constant c_χ drops out due to the antisymmetrization.

For three lightlike Wilson lines the calculation of the diagrams in Fig. 6 can also be considered directly using a conformal gauge. To do this we should use the conformal gauge from Eq. (A8), rather than the one in Eq. (55). This conformal gauge has no $D_{\tau i}$ or $D_{i\tau}$ mixing terms and is identical to Feynman gauge for $D_{\tau\tau}$ in d dimensions. The lack of mixing terms immediately implies that Fig. 6(a) is
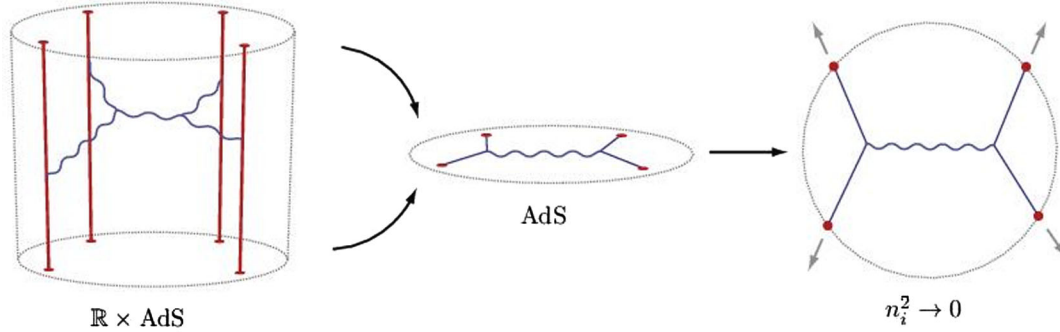
FIG. 7 (color online).   After doing all the τ-integrals, the computation of certain diagrams dimensionally reduces from $\mathbb{R} \times$ AdS to AdS. In the limit where the charges approach the boundary $n_i^2 \to 0$, we obtain a Witten diagram.

zero, a result that is only seen in Feynman gauge by direct computation [37]. For the remaining diagrams, Fig. 6(b) and 6(c), the calculation is identical to the one in Feynman gauge, so the sum of these diagrams is zero just as it is there [37,66].

VIII. RELATION TO WITTEN DIAGRAMS IN THE LIGHTLIKE LIMIT

Finally, let us comment on an interesting formal similarity between the perturbation expansion for $\Gamma_{\mathrm{cusp}}(n_i)$ in the lightlike limit and the Witten diagram expansion for AdS scattering amplitudes, which has been well studied in the AdS/CFT literature [69–74]. Recall from the previous section that diagrams with at most one gluon attached to each line involve only τ-independent modes of the gauge field. After performing integrals in the τ-direction, they become AdS scattering amplitudes in a gauge theory containing an adjoint scalar, which is sourced by each charge. As the parton directions become lightlike $n_i^2 \to 0$, the corresponding charges move off to the boundary of AdS. We are left, at least formally, with a boundary-to-boundary scattering amplitude—a Witten diagram (Fig. 7).

We could have anticipated some relation to Witten diagrams simply from the geometry. Our realization of AdS_3 as a hyperboloid inside $\mathbb{R}^{1,3}$ is known in the AdS/CFT literature as the *embedding space* (or sometimes *covering space*) formalism [75–80]. Its utility is that the isometries of AdS (and conformal transformations of its boundary) become linearly realized Lorentz transformations of the embedding space, an observation that dates back to Dirac [75]. Here, we arrived at this formalism from the other direction, beginning in Minkowski space, and finding that AdS geometry appears naturally.

A possible correspondence between Feynman diagrams for $\Gamma_{\mathrm{cusp}}(n_i)$ and Witten diagrams is complicated by several issues. Firstly, as we argued extensively in Sec. III, choosing proper boundary conditions in AdS is crucial for capturing the correct physics. For example, our scalar bulk-to-bulk propagator is the potential we computed in Eq. (26),

$$D_{BB}(n_1, n_2) = \frac{1}{4\pi^2}(\pi + i\beta_{12})\coth\beta_{12}. \quad (66)$$

Recall that this solves Laplace's equation in the presence of a constant charge density, so does not correspond to the usual bulk-to-bulk scalar propagator, which solves the homogeneous Laplace's equation in AdS. In the limit that one of the directions n_1 becomes lightlike, we also obtain an unorthodox boundary-to-bulk propagator

$$
\begin{aligned}
D_{\partial B}(n_1, n_2) &= \lim_{|n_1| \to 0} D_{BB}(n_1, n_2) \\
&= \lim_{|n_1| \to 0} \frac{i}{4\pi^2}\left(-\log|n_1| + \log\frac{n_1 \cdot n_2}{|n_2|}\right). \quad (67)
\end{aligned}
$$

This is divergent as $|n_1| \to 0$, a reflection of the collinear singularities that arise in this limit.[6]

Contributions to Γ also differ from traditional Witten diagrams in their contours of integration. For Witten diagrams, one performs bulk integrals over AdS, whereas Feynman integrals involve all of Minkowski space, so should incorporate both copies of AdS and dS as well (Fig. 3).

To use Witten diagrams for computing Γ, one must account for all of the above issues. Nevertheless, the possible applicability of AdS amplitude technology is encouraging. Witten diagrams have been well studied, and recently new techniques involving Mellin representations have substantially improved efficiency of computation [81–85].

---

[6]Its form is perhaps reminiscent of the traditional boundary-to-bulk propagator for a scalar with an infinitesimal mass

$$D_{\partial B}(n_1, n_2) \overset{?}{\sim} \lim_{\Delta \to 0} \frac{i}{4\pi^2} \frac{1}{\Delta}\left(\frac{n_1 \cdot n_2}{|n_2|}\right)^{\Delta} \quad (68)$$

where the mass is related to Δ via the usual AdS/CFT dictionary, $m^2 R_{\mathrm{AdS}}^2 = \Delta(\Delta - 2)$. One might speculate that in a calculation where the $-\log|n_i|$ singularities are regulated and cancel appropriately, Eq. (68) might be an acceptable form for the boundary-to-bulk propagator.

As an example, the gauge-boson exchange diagram depicted in Fig. 7 was first computed with traditional boundary conditions over a decade ago [72–74]. The answer is a nontrivial sum of so-called D-functions $D_{\Delta_1,\Delta_2,\Delta_3,\Delta_4}(u, v)$, where u and v are conformal cross-ratios. Formally, this diagram contributes to the regular anomalous dimension $\gamma(\alpha_s, \{n_i \cdot n_j\})$ in Eq. (12) at three loops, with a color structure $f^{abe}f^{cde}T_i^a T_j^b T_k^c T_l^d$. While we have understood using conformal gauge why $\Gamma_{\text{cusp}}(n_i)$ should have a pairwise structure up to two loops, we see no *a priori* reason that this structure should persist to higher orders. We interpret the fact that the diagram in Fig. 7 is nonzero as an indication that $\gamma(\alpha_s, \{n_i \cdot n_j\})$ might very well have nontrivial conformal cross-ratio dependence. Very recently, two papers have appeared [42,43] which propose that additional constraints on the conformal cross-ratio dependence of the soft anomalous dimension follow from consideration of the Regge limit. Perhaps by using tools developed for Witten diagrams, the three-loop anomalous dimension can be calculated exactly, hopefully resolving the controversy in *feature 6*.

IX. CONCLUSIONS

In this paper we have discussed how properties of operators $\mathcal{W}$ built from N Wilson lines can be understood in radial coordinates. These operators appear in high-energy collisions that produce jets, where the lines extend out from the location of the hard interaction, taken to be the origin. In radial coordinates, $\mathbb{R} \times \text{AdS}$, the direction of the Wilson lines are specified by points in Euclidean AdS_3 and motion along any of the Wilson lines corresponds to time translations of $\tau \in \mathbb{R}$.

We have demonstrated that many of the key properties of anomalous dimensions of these operators have an intuitive and simple description in terms of these static charges in AdS. In particular: the dependence on cusp angles β_{ij} just corresponds to the geometric distance between the lines in AdS; the one-loop anomalous dimension of $\mathcal{W}$ is given by a classical energy computation on AdS (with special care given to boundary conditions).

There is an intuitive physical picture associated to the real and imaginary parts of the anomalous dimension. This picture leads to an intriguing analogy between the at most linear growth of imaginary energy with separation in AdS, guaranteed by the at most linear growth of the anomalous dimensions with cusp angles, and the linear dependence of energy on separation for charges in gauge theories, which is associated with the flux-tube picture of confinement.

To fully exploit the physical picture arising in $\mathbb{R} \times \text{AdS}$ we introduced a class of gauges, referred to as conformal gauges. In these gauges, there is no kinetic mixing between temporal components of the gauge field, A_τ, and spatial components, A_i. Conformal gauges are formulated in position space in d dimensions, so that they are suitable for

calculations using dimensional regularization. Conformal gauges in $\mathbb{R} \times \text{AdS}$ are effectively the analog of Feynman gauge in flat space, and simplify some perturbative computations involving Wilson lines. Since all Wilson lines are only sources for A_τ, the absence of mixing directly implies that one only has to consider scalar exchange at leading orders in perturbation theory. In particular graphs involving three-gluon or four-gluon vertices may vanish simply from the absence of $(A_\tau)^3$ and $(A_\tau)^4$ interactions in QCD. We have demonstrated this explicitly by considering a two-loop computation involving three timelike Wilson lines, and showing that it reduces to a one-loop computation with counterterm insertions. For three lightlike Wilson lines we have also shown that a suitable conformal gauge simplifies this calculation by making it explicit that the most complicated diagram involving the three-gluon vertex vanishes.

Many avenues remain open to future exploration, and we have only briefly touched on a few of them. In the limit where one or more Wilson lines become lightlike, extra ultraviolet and infrared divergences appear, and new features emerge in the anomalous dimension of $\mathcal{W}$, such as dependence on the renormalization group scale μ. While we have formulated a suitable conformal gauge for use with lightlike lines, we have not explored in detail many interesting computations, such as the two-loop anomalous dimension from two lightlike lines, or graphs occurring in soft functions that have real radiation. Many interesting questions only appear for $\mathcal{W}$ with four lines taken at three loops and beyond, such as possible dependence of the anomalous dimension on conformal cross-ratios. We anticipate that the use of conformal gauges will be a powerful technique for analyses which seek to definitively answer questions which appear at this order.

We have also observed a relationship between diagrams with multiple Wilson lines and Witten diagrams, which have been studied extensively in the context of the AdS/CFT correspondence. There is hope that technology developed for computing these Witten diagrams can be used directly for calculations about Wilson lines, with direct application to jet physics, and possibly also to improved understanding of the structure of amplitudes in gauge theories.

Córdova, F. Denef, R. Loganayagam, and D. Poland for discussions.

APPENDIX A: GENERAL CLASS OF CONFORMAL GAUGES

The most general possible form of the gauge transformation one-form is[7]

$$\Lambda_\mu(y, x) = \frac{\kappa_d}{(|x||y|)^{d/2-1}} [x_\mu g_1(\alpha, \beta) + y_\mu g_2(\alpha, \beta)],$$

where $\alpha \equiv \dfrac{x \cdot y}{|x||y|}, \qquad \beta \equiv \dfrac{|y|}{|x|}$,   (A1)

and $g_{1,2}(\alpha, \beta)$ are functions to be specified. Equation (48) yields the propagator

$$D_{\mu\nu}(x, y) = \frac{\kappa_d}{(|x||y|)^{d/2-1}} \left[g_{\mu\nu} A + \frac{x_\mu x_\nu}{x^2} B + \frac{y_\mu y_\nu}{y^2} C \right.$$
$$\left. + \frac{x_\mu y_\nu}{|x||y|} E + \frac{y_\mu x_\nu}{x \cdot y} Z \right],$$ (A2)

where we have

$$A = -[2\alpha - \beta - \beta^{-1}]^{1-d/2} + g_2 + \bar{g}_2,$$
$$B = \beta^{-1} g_1^{(1,0)} + (1 - d/2)\bar{g}_2 - \alpha \bar{g}_2^{(1,0)} + \beta^{-1} \bar{g}_2^{(0,1)},$$
$$C = \beta \bar{g}_1^{(1,0)} + (1 - d/2)g_2 - \alpha g_2^{(1,0)} + \beta g_2^{(0,1)},$$
$$E = g_1^{(0,1)} + \bar{g}_1^{(0,1)} + (1 - d/2)(\beta^{-1} g_1 + \beta \bar{g}_1)$$
$$\quad - \alpha(\beta^{-1} g_1^{(1,0)} + \beta \bar{g}_1^{(1,0)}),$$
$$Z = \alpha g_2^{(1,0)} + \alpha \bar{g}_2^{(1,0)},$$ (A3)

with the definitions $\bar{g}_i(\alpha, \beta) = g_i(\alpha, \beta^{-1})$, $g_i^{(1,0)} = \partial g_i(\alpha, \beta)/\partial \alpha$, $g_i^{(0,1)} = \partial g_i(\alpha, \beta)/\partial \beta$, $\bar{g}_i^{(0,1)} = \partial g_i \times (\alpha, \beta^{-1})/\partial \beta^{-1}$, etc. The conformal gauge conditions, which ensure there is no mixing between time and spatial directions in $\mathbb{R} \times \text{AdS}$, are $x^\mu D_{\mu\nu}(x, y)A^\nu(y) = 0$ when $y_\nu A^\nu(y) = 0$, and $A^\mu(x)D_{\mu\nu}(x, y)y^\nu = 0$ when $x_\mu A^\mu(x) = 0$. These require

$$A + B + Z = 0, \qquad B = C,$$ (A4)

which are two differential equations for the functions g_1 and g_2. Substituting Eq. (A4) into Eq. (A2) yields the general result for the conformal gauge propagator

---

[7]More general forms are possible if we introduce one or more additional fixed vectors in the gauge transformation, such as a v^μ where $v^2 = 1$.

$$\tilde{D}_{\mu\nu}(x, y) = \frac{\kappa_d}{(|x||y|)^{d/2-1}} \left[\left(g_{\mu\nu} - \frac{x_\mu x_\nu}{x^2} - \frac{y_\mu y_\nu}{y^2} \right. \right.$$
$$\left. + \frac{x \cdot y x_\mu y_\nu}{x^2 y^2} \right) A + \left(\frac{y_\mu x_\nu}{x \cdot y} - \frac{x_\mu x_\nu}{x^2} - \frac{y_\mu y_\nu}{y^2} \right)$$
$$+ \frac{x \cdot y x_\mu y_\nu}{x^2 y^2} Z + \frac{x \cdot y x_\mu y_\nu}{x^2 y^2} \left(\frac{E}{\alpha} - A - Z \right) \bigg].$$
       (A5)

The first two tensor structures are spatial (angular), while the latter is temporal (radial). Using Eq. (A4) and (A3) we can write

$$\frac{E}{\alpha} - A - Z = -(2\alpha - \beta - \beta^{-1})^{1-d/2}$$
$$+ [(2 - d/2)(g_2 + \bar{g}_2)$$
$$+ \beta g_2^{(0,1)} + \beta^{-1} \bar{g}_2^{(0,1)}]$$
$$+ \alpha^{-1}[(1 - d/2)(\beta^{-1} g_1 + \beta \bar{g}_1)$$
$$+ g_1^{(0,1)} + \bar{g}_1^{(0,1)}],$$ (A6)

where the first term is the result from Feynman gauge and the last two terms are induced by the gauge transformation.

To consider the lightlike limit for x and y we take $x^\mu = \lambda_1 n_1^\mu$ and $y^\mu = \lambda_2 n_2^\mu$, where without loss of generality we take $\lambda_i > 0$ and send $n_1^2 = n_2^2 \to 0$. This leaves $\beta = \lambda_2/\lambda_1$ fixed and sends $\alpha \to \infty$. For the propagator between points on two lightlike Wilson lines only the last term in Eq. (A5) contributes,

$$n_1^\mu n_2^\nu \tilde{D}_{\mu\nu}(x, y) = \kappa_d n_1 \cdot n_2 \lim_{n_i^2 \to \infty} (\lambda_1^2 \lambda_2^2 n_1^2 n_2^2)^{1/2 - d/4}$$
$$\times \left[\frac{E}{\alpha} - A - Z \right].$$ (A7)

To ensure this gives the same result as Feynman gauge we can choose a conformal gauge where

$$g_1(\alpha, \beta) = -\alpha \beta g_2(\alpha, \beta),$$ (A8)

which makes $E/\alpha - A - Z = -(2\alpha - \beta - \beta^{-1})^{1-d/2}$. Equation (A7) then becomes

$$n_1^\mu n_2^\nu \tilde{D}_{\mu\nu}(x, y) = -\kappa_d n_1 \cdot n_2 (2n_1 \cdot n_2 \lambda_1 \lambda_2)^{1-d/2},$$ (A9)

which is the same as the Feynman gauge result. The $A + B + Z = 0$ and $B = C$ no mixing conditions for this case becomes

$$\beta g_2^{(0,1)} + (2 - d/2)g_2 = (2\alpha - \beta - \beta^{-1})^{1-d/2},$$ (A10)

which implies

$$g_2(\alpha, \beta) = \beta^{d/2-2}(\alpha^2 - 1)^{1-d/2}(\beta - \alpha)_2 F_1$$
$$\times \left(\frac{1}{2}, \frac{d}{2} - 1, \frac{3}{2}, \frac{(\alpha - \beta)^2}{\alpha^2 - 1} \right) + \beta^{d/2-2} h(\alpha),$$
       (A11)

with an arbitrary function $h(\alpha)$ that still must be fixed to fully specify the gauge. Using Eqs. (A3), (A8), and (A11) determine the spatial terms in the conformal gauge-boson propagator in Eq. (A5). It is straightforward to verify that the propagator is nonsingular in the limit $d \to 4$.

APPENDIX B: GHOSTS IN CONFORMAL GAUGE

In position space the Feynman rules for ghosts are more easily represented with a "ghost field" G_μ^{abc} which is the product of a ghost propagator and ghost-gluon vertex. For the gauge transformation in Eq. (48) the appropriate ghost field is [86]

$$
\begin{aligned}
G_\mu^{abc}(y, x) = -ig f^{abc} [\partial_y^\nu D_{\mu\nu}^F(x, y) \\
+ (\partial_\mu^x \partial_\nu^x - g_{\mu\nu}\Box_x)\Lambda^\nu(y, x)], \quad \text{(B1)}
\end{aligned}
$$

where $D_{\mu\nu}^F$ is the Feynman-gauge gluon propagator from Eq. (47) and $\Lambda^\nu(y, x)$ is the one-form appearing in the gauge transformed gluon propagator $D_{\mu\nu}$. This result can be used for any member of the general class of conformal gauges discussed in App. A.

[1] J. C. Collins, D. E. Soper, and G. Sterman, Adv. Ser. Dir. High Energy Phys. **5**, 1 (1988).
[2] G. Sterman, arXiv:hep-ph/9606312.
[3] C. W. Bauer, S. Fleming, and M. E. Luke, Phys. Rev. D **63**, 014006 (2000).
[4] C. W. Bauer, S. Fleming, D. Pirjol, and I. W. Stewart, Phys. Rev. D **63**, 114020 (2001).
[5] C. W. Bauer and I. W. Stewart, Phys. Lett. B **516**, 134 (2001).
[6] C. W. Bauer, D. Pirjol, and I. W. Stewart, Phys. Rev. D **65**, 054022 (2002).
[7] C. W. Bauer, S. Fleming, D. Pirjol, I. Z. Rothstein, and I. W. Stewart, Phys. Rev. D **66**, 014017 (2002).
[8] L. F. Alday and J. M. Maldacena, J. High Energy Phys. 06 (2007) 064.
[9] G. Korchemsky, J. Drummond, and E. Sokatchev, Nucl. Phys. **B795**, 385 (2008).
[10] A. Brandhuber, P. Heslop, and G. Travaglini, Nucl. Phys. **B794**, 231 (2008).
[11] J. Drummond, J. Henn, G. Korchemsky, and E. Sokatchev, Nucl. Phys. **B795**, 52 (2008).
[12] J. Drummond, J. Henn, G. Korchemsky, and E. Sokatchev, Phys. Lett. B **662**, 456 (2008).
[13] Z. Bern, L. Dixon, D. Kosower, R. Roiban, M. Spradlin *et al.*, Phys. Rev. D **78**, 045007 (2008).
[14] J. Drummond, J. Henn, G. Korchemsky, and E. Sokatchev, Nucl. Phys. **B815**, 142 (2009).
[15] N. Berkovits and J. Maldacena, J. High Energy Phys. 09 (2008) 062.
[16] A. V. Manohar, Phys. Rev. D **68**, 114019 (2003).
[17] C. W. Bauer and M. D. Schwartz, Phys. Rev. D **76**, 074004 (2007).
[18] C. W. Bauer and M. D. Schwartz, Phys. Rev. Lett. **97**, 142001 (2006).
[19] S. Fleming, A. H. Hoang, S. Mantry, and I. W. Stewart, Phys. Rev. D **77**, 114003 (2008).
[20] R. Kelley and M. D. Schwartz, Phys. Rev. D **83**, 045022 (2011).
[21] G. P. Korchemsky, G. Oderda, and G. Sterman, arXiv:hep-ph/9708346.
[22] M. D. Schwartz, Phys. Rev. D **77**, 014026 (2008).

[23] C. W. Bauer, S. Fleming, C. Lee, and G. Sterman, Phys. Rev. D **78**, 034027 (2008).
[24] T. Becher and M. Neubert, J. High Energy Phys. 06 (2009) 081.
[25] T. Becher and M. D. Schwartz, J. High Energy Phys. 02 (2010) 040.
[26] R. Kelley and M. D. Schwartz, Phys. Rev. D **83**, 033001 (2011).
[27] S. D. Ellis, C. K. Vermilion, J. R. Walsh, A. Hornig, and C. Lee, J. High Energy Phys. 11 (2010) 101.
[28] T. T. Jouttenus, I. W. Stewart, F. J. Tackmann, and W. J. Waalewijn, Phys. Rev. D **83**, 114030 (2011).
[29] R. A. Brandt, F. Neri, and M.-a. Sato, Phys. Rev. D **24**, 879 (1981).
[30] V. Ahrens, T. Becher, M. Neubert, and L. L. Yang, Phys. Rev. D **79**, 033013 (2009).
[31] G. Korchemsky and A. Radyushkin, Nucl. Phys. **B283**, 342 (1987).
[32] L. F. Alday and J. M. Maldacena, J. High Energy Phys. 11 (2007) 019.
[33] A. Vogt, S. Moch, and J. Vermaseren, Nucl. Phys. **B691**, 129 (2004).
[34] C. W. Bauer and A. V. Manohar, Phys. Rev. D **70**, 034024 (2004).
[35] J.-y. Chiu, R. Kelley, and A. V. Manohar, Phys. Rev. D **78**, 073006 (2008).
[36] J.-y. Chiu, A. Fuhrer, R. Kelley, and A. V. Manohar, Phys. Rev. D **80**, 094013 (2009).
[37] S. Aybat, L. J. Dixon, and G. F. Sterman, Phys. Rev. Lett. **97**, 072001 (2006).
[38] T. Becher and M. Neubert, Phys. Rev. Lett. **102**, 162001 (2009).
[39] E. Gardi and L. Magnea, J. High Energy Phys. 03 (2009) 079.
[40] Z. Bern, J. Carrasco, L. J. Dixon, H. Johansson, and R. Roiban, Phys. Rev. D **78**, 105019 (2008).
[41] L. J. Dixon, E. Gardi, and L. Magnea, Proc. Sci., RADCOR2009 (2010) 007.
[42] V. Del Duca, C. Duhr, E. Gardi, L. Magnea, and C. D. White, arXiv:1109.3581 [J. High Energy Phys. (to be published)].

[43] V. Del Duca, C. Duhr, E. Gardi, L. Magnea, and C. D. White, arXiv:1108.5947.

[44] A. V. Belitsky, A. S. Gorsky, and G. P. Korchemsky, Nucl. Phys. **B667**, 3 (2003).

[45] V. Braun, G. Korchemsky, and D. Mueller, Prog. Part. Nucl. Phys. **51**, 311 (2003).

[46] L. N. Lipatov, arXiv:hep-th/9311037.

[47] L. D. Faddeev and G. P. Korchemsky, Phys. Lett. B **342**, 311 (1995).

[48] G. P. Korchemsky, Nucl. Phys. **B443**, 255 (1995).

[49] A. V. Manohar and M. B. Wise, Cambridge Monogr. Part. Phys., Nucl. Phys., Cosmol. **10**, 1 (2000).

[50] P. Di Francesco, P. Mathieu, and D. Senechal, *Conformal Field Theory* (Springer, New York, USA, 1997), p. 890.

[51] G. Parisi, Phys. Lett. B **90**, 295 (1980).

[52] G. Sterman, Nucl. Phys. **B281**, 310 (1987).

[53] L. Magnea and G. Sterman, Phys. Rev. D **42**, 4222 (1990).

[54] T. O. Eynck, E. Laenen, and L. Magnea, J. High Energy Phys. 06 (2003) 057.

[55] D. Yennie, S. C. Frautschi, and H. Suura, Ann. Phys. (N.Y.) **13**, 379 (1961).

[56] J. Gatheral, Phys. Lett. B **133**, 90 (1983).

[57] J. Frenkel and J. Taylor, Nucl. Phys. **B246**, 231 (1984).

[58] E. Gardi, E. Laenen, G. Stavenga, and C. D. White, J. High Energy Phys. 11 (2010) 155.

[59] A. Mitov, G. Sterman, and I. Sung, Phys. Rev. D **82**, 096010 (2010).

[60] C. D. White, J. High Energy Phys. 05 (2011) 060.

[61] R. Akhoury, R. Saotome, and G. Sterman, Phys. Rev. D **84**, 104040 (2011).

[62] S. G. Naculich and H. J. Schnitzer, J. High Energy Phys. 05 (2011) 087.

[63] T. Sjostrand, S. Mrenna, and P. Z. Skands, J. High Energy Phys. 05 (2006) 026.

[64] R. Sundrum, arXiv:hep-ph/9702306.

[65] S. Leupold and H. Weigert, Phys. Rev. D **54**, 7695 (1996).

[66] S. M. Aybat, L. J. Dixon, and G. F. Sterman, Phys. Rev. D **74**, 074004 (2006).

[67] A. Mitov, G. F. Sterman, and I. Sung, Phys. Rev. D **79**, 094015 (2009).

[68] A. Ferroglia, M. Neubert, B. D. Pecjak, and L. L. Yang, J. High Energy Phys. 11 (2009) 062.

[69] E. Witten, Adv. Theor. Math. Phys. **2**, 253 (1998).

[70] D. Z. Freedman, S. D. Mathur, A. Matusis, and L. Rastelli, Nucl. Phys. **B546**, 96 (1999).

[71] D. Z. Freedman, S. D. Mathur, A. Matusis, and L. Rastelli, Phys. Lett. B **452**, 61 (1999).

[72] E. D'Hoker and D. Z. Freedman, Nucl. Phys. **B544**, 612 (1999).

[73] E. D'Hoker, D. Z. Freedman, S. D. Mathur, A. Matusis, and L. Rastelli, Nucl. Phys. **B562**, 330 (1999).

[74] E. D'Hoker, D. Z. Freedman, and L. Rastelli, Nucl. Phys. **B562**, 395 (1999).

[75] P. A. Dirac, Ann. Math. **37**, 429 (1936).

[76] G. Mack and A. Salam, Ann. Phys. (N.Y.) **53**, 174 (1969), http://www.sciencedirect.com/science/article/pii/0003491669902784.

[77] D. Boulware, L. Brown, and R. Peccei, Phys. Rev. D **2**, 293 (1970).

[78] S. Ferrara, A. Grillo, and R. Gatto, Ann. Phys. (N.Y.) **76**, 161 (1973).

[79] S. Weinberg, Phys. Rev. D **82**, 045031 (2010).

[80] M. S. Costa, J. Penedones, D. Poland, and S. Rychkov, J. High Energy Phys. 11 (2011) 071.

[81] G. Mack, arXiv:0907.2407.

[82] G. Mack, dedicated to professor Ivan Todorov on the occasion of his 75th anniversary, arXiv:0909.1024.

[83] J. Penedones, J. High Energy Phys. 03 (2011) 025.

[84] M. F. Paulos, J. High Energy Phys. 10 (2011) 074.

[85] A. Fitzpatrick, J. Kaplan, J. Penedones, S. Raju, and B. C. van Rees, J. High Energy Phys. 11 (2011) 095.

[86] H. Cheng and E.-C. Tsai, Phys. Rev. D **36**, 3196 (1987).

[87] J. Gallicchio and M. D. Schwartz, Phys. Rev. Lett. **105**, 022001 (2010).